SIAM J. SCI. COMPUT.
Vol. 37, No. 5, pp. S264–S290
© 2015 Society for Industrial and Applied Mathematics

A DOMAIN DECOMPOSITION METHOD FOR THE STEADY-STATE NAVIER–STOKES–DARCY MODEL WITH BEAVERS–JOSEPH INTERFACE CONDITION*

XIAOMING HE†, JIAN LI‡, YANPING LIN§, AND JU MING¶

Abstract. This paper proposes and analyzes a Robin-type multiphysics domain decomposition method (DDM) for the steady-state Navier–Stokes–Darcy model with three interface conditions. In addition to the two regular interface conditions for the mass conservation and the force balance, the Beavers–Joseph condition is used as the interface condition in the tangential direction. The major mathematical difficulty in adopting the Beavers–Joseph condition is that it creates an indefinite leading order contribution to the total energy budget of the system [Y. Cao et al., *Comm. Math. Sci.*, 8 (2010), pp. 1–25; Y. Cao et al., *SIAM J. Numer. Anal.*, 47 (2010), pp. 4239–4256]. In this paper, the well-posedness of the Navier–Stokes–Darcy model with Beavers–Joseph condition is analyzed by using a branch of nonsingular solutions. By following the idea in [Y. Cao et al., *Numer. Math.*, 117 (2011), pp. 601–629], the three physical interface conditions are utilized together to construct the Robin-type boundary conditions on the interface and decouple the two physics which are described by Navier–Stokes and Darcy equations, respectively. Then the corresponding multiphysics DDM is proposed and analyzed. Three numerical experiments using finite elements are presented to illustrate the features of the proposed method and verify the results of the theoretical analysis.

Key words. Navier–Stokes–Darcy flow, Beavers–Joseph interface condition, domain decomposition method, finite elements

AMS subject classifications. 65N55, 65N12, 65N30, 76D05, 76S05

DOI. 10.1137/140965776

1. Introduction.

In the past decade many scientists and engineers have investigated the Stokes-Darcy models for the coupling of fluid flows and porous media flows. Different numerical methods, have been developed and analyzed such as the coupled finite element methods [18, 25, 28, 31, 44, 66, 71, 78, 96], domain decomposition methods (DDMs) [13, 10, 16, 17, 26, 34, 35, 37, 36, 39, 45, 65, 68, 107], Lagrange multiplier methods [5, 51, 52, 67, 74], multigrid methods [3, 11, 12, 83, 113, 114, 115], discontinuous Galerkin methods [56, 70, 80, 94, 95], mortar finite element methods [43, 49, 48, 50, 57], least square methods [41, 75, 85, 106], partitioned time stepping methods [84, 99], boundary integral method [9, 90, 105], multiple-time-step methods [97, 100], stabilization methods [29, 86, 89], and many others [23, 27, 32, 40, 53, 54, 60, 61, 72, 81, 101, 110].

The quick development of this research area is due to its many applications in different real world problems, which include, but are not limited to, the groundwater

*Received by the editors April 18, 2014; accepted for publication (in revised form) March 24, 2015; published electronically October 29, 2015. This work was partially supported by NSF grant DMS-1418624, NSF of China (11371031, 91330104), and GRF of HKSAR (501012).
http://www.siam.org/journals/sisc/37-5/96577.html
†Department of Mathematics and Statistics, Missouri University of Science and Technology, Rolla, MO 65409 (hex@mst.edu).
‡Corresponding author. Research Center for Computational Science, Northwestern Polytechnical University, Xi'an, 710072, People's Republic of China, and Department of Mathematics, Baoji University of Arts and Sciences, Baoji, 721007, People's Republic of China (jiaaanli@gmail.com).
§Department of Applied Mathematics, Hong Kong Polytechnic University, Hung Hom, Hong Kong (yanping.lin@polyu.edu.hk).
¶Beijing Computational Science Research Center, Beijing, 100084, People's Republic of China (jming@csrc.ac.cn).

system in karst aquifers [7, 18, 19], flow in vuggy porous media or around a horizontal wellbore [2, 4, 59, 63, 69, 73, 88, 111, 112], interaction between surface and subsurface flows [33, 37, 56, 74], field-flow fractionation for the separation and characterization of proteins, polymers, and other macromolecules [14, 47, 93, 102], industrial filtrations [42, 62, 87], blood motion in lungs, solid tumors, and vessels [92, 104], remediation of soils by means of bacterial colonies [1], meshy zone in alloy solidification [46, 103, 108, 109], spontaneous combustion of coal stockpiles [98], heat transfer in walls with fibrous insulation [82, 91], and topology optimization [58].

However, most of the existing works are devoted to the linear Stokes–Darcy model. Hence, recently scientists began studying the more physically faithful Navier–Stokes–Darcy model [6, 12, 15, 21, 22, 20, 30, 56]. In this paper, we will extend the previous work for the linear Stokes–Darcy model in [16] to the multiphysics domain decomposition method (DDM) for the steady-state Navier–Stokes–Darcy model with Beavers–Joseph condition. A branch of nonsingular solutions is utilized for the analysis to provide Proposition 4.1, which shows the well-posedness of the coupled nonlinear weak formulation. Then following the idea in [16], we will propose and analyze a physics-based DDM for the Navier–Stokes–Darcy model based on some Robin-type boundary conditions constructed from the following three physical interface conditions: the conservation of mass, the balance of forces, and the Beavers–Joseph condition. The physics-based DDMs are different from the traditional ones in the sense that they focus on decomposing different physical domains by directly using the given physical interface conditions. As expected, a new, major difficulty arises from the nonlinear advection in the Navier–Stokes equations and its interaction with the Beavers–Joseph interface condition even though the development and the analysis of the proposed method fall within the same framework of [16]. When the weak formulation is constructed, an additional consistent term is added to the trilinear form in order to ensure (3.4) in a space which is large enough to include both the coupled weak solution and the domain decomposition solutions. This property will play a key role in the convergence analysis of the DDM. Furthermore, this paper provides more realistic numerical experiments than those of [16].

The rest of paper is organized as follows. In section 2, we introduce the steady-state Navier–Stokes–Darcy model with the Beavers–Joseph interface condition. In section 3, a coupled weak formulation is proposed, and the trilinear form utilized in this formulation is analyzed. In section 4, a branch of nonsingular solutions is studied for the well-posedness of the coupled weak formulation. In section 5, a multiphysics DDM is proposed based on the decoupled Navier–Stokes and Darcy systems by using Robin-type boundary conditions arising from the three interface conditions. Then this method is analyzed in section 6. In section 7, we present three numerical examples to illustrate the features of the proposed method. Finally, we conclude in section 8.

2. Steady-state Navier–Stokes–Darcy model. In this section we introduce the following coupled Navier–Stokes–Darcy model on a bounded domain $\Omega = \Omega_D \cup \Omega_S \subset \mathbb{R}^d$ $(d = 2, 3)$; see Figure 1.

In the porous media region Ω_D, the flow is governed by the Darcy system

$$\overrightarrow{u}_D = -\mathbb{K}\nabla\phi_D, \tag{2.1}$$

$$\nabla \cdot \overrightarrow{u}_D = f_D. \tag{2.2}$$

Here, $\overrightarrow{u}_D$ is the fluid discharge rate in the porous media, $\mathbb{K}$ is the hydraulic conductivity tensor, f_D is a sink/source term, and ϕ_D is the hydraulic head defined as

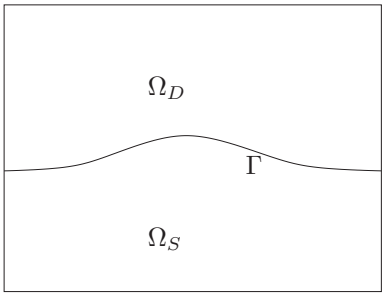

FIG. 1. *A sketch of the porous median domain Ω_D, fluid domain Ω_S, and the interface Γ.*

$z + \frac{p_D}{\rho g}$, where p_D denotes the dynamic pressure, z the height, ρ the density, and g the gravitational acceleration. We will consider the following second order formulation, which eliminates $\overrightarrow{u}_D$ in the Darcy system:

$$-\nabla \cdot (\mathbb{K}\nabla\phi_D) = f_D. \tag{2.3}$$

In the fluid region Ω_S, the fluid flow is assumed to be governed by the Navier–Stokes equations

$$\overrightarrow{u}_S \cdot \nabla \overrightarrow{u}_S - \nabla \cdot \mathbb{T}(\overrightarrow{u}_S, p_S) = \overrightarrow{f}_S, \tag{2.4}$$

$$\nabla \cdot \overrightarrow{u}_S = 0, \tag{2.5}$$

where $\overrightarrow{u}_S$ is the fluid velocity, p_S is the kinematic pressure, $\overrightarrow{f}_S$ is the external body force, ν is the kinematic viscosity of the fluid, $\mathbb{T}(\overrightarrow{u}_S, p_S) = 2\nu\mathbb{D}(\overrightarrow{u}_S) - p_S\mathbb{I}$ is the stress tensor, and $\mathbb{D}(\overrightarrow{u}_S) = (\nabla\overrightarrow{u}_S + \nabla^T\overrightarrow{u}_S)/2$ is the deformation tensor.

Let $\Gamma = \overline{\Omega}_D \cap \overline{\Omega}_S$ denote the interface between the fluid and porous media regions. On the interface Γ, we impose the following three interface conditions:

$$\overrightarrow{u}_S \cdot \overrightarrow{n}_S = -\overrightarrow{u}_D \cdot \overrightarrow{n}_D, \tag{2.6}$$

$$-\overrightarrow{n}_S \cdot (\mathbb{T}(\overrightarrow{u}_S, p_S) \cdot \overrightarrow{n}_S) + \frac{1}{2}\overrightarrow{u}_S \cdot \overrightarrow{u}_S = g(\phi_D - z), \tag{2.7}$$

$$-\boldsymbol{\tau}_j \cdot (\mathbb{T}(\overrightarrow{u}_S, p_S) \cdot \overrightarrow{n}_S) = \frac{\alpha\nu\sqrt{\mathbf{d}}}{\sqrt{\mathrm{trace}(\prod)}}\boldsymbol{\tau}_j \cdot (\overrightarrow{u}_S - \overrightarrow{u}_D), \tag{2.8}$$

where $\overrightarrow{n}_S$ and $\overrightarrow{n}_D$ denote the unit outer normal to the fluid and the porous media regions at the interface Γ, respectively; $\boldsymbol{\tau}_j$ $(j = 1, \ldots, d-1)$ denote mutually orthogonal unit tangential vectors to the interface Γ, α is the Beavers–Joseph constant, and $\prod = \frac{\mathbb{K}\nu}{g}$.

The first interface condition can be easily obtained from the conservation of mass. The second condition describes the balance of the forces [22, 30]. The third condition is referred to as the Beavers–Joseph (BJ) interface condition [8]. The BJ interface condition creates an indefinite leading order contribution to the total energy budget of the system, which causes a major mathematical difficulty in adopting the BJ interface condition [19, 18]. More theoretical support for the BJ condition can be found in [24].

In this paper, for simplification we assume that the hydraulic head ϕ_D and the fluid velocity $\overrightarrow{u}_S$ satisfy the homogeneous Dirichlet boundary condition except on Γ, i.e., $\phi_D = 0$ on the boundary $\partial\Omega_D\backslash\Gamma$and $\overrightarrow{u}_S = 0$ on the boundary $\partial\Omega_S\backslash\Gamma$. Without loss of generality, we also assume that $\mathbb{K}$ is isotropic.

3. Coupled weak formulation. Let $(\cdot,\cdot)_D$ denote the L^2 inner product on the domain D ($D = \Omega_S$ or Ω_D), and let $\langle\cdot,\cdot\rangle$ denote the L^2 inner product on the interface Γ or the duality pairing between $(H_{00}^{1/2}(\Gamma))'$ and $H_{00}^{1/2}(\Gamma)$. Define the spaces

$$\begin{aligned} X_S &= \{\overrightarrow{v} \in [H^1(\Omega_S)]^d \mid \overrightarrow{v} = 0 \text{ on } \partial\Omega_S\backslash\Gamma\},\\ Q_S &= L^2(\Omega_S),\\ X_D &= \{\psi \in H^1(\Omega_D) \mid \psi = 0 \text{ on } \partial\Omega_D\backslash\Gamma\}. \end{aligned}$$

Let $\lambda = \frac{1}{\nu}$. Then the weak formulation of the coupled Navier–Stokes–Darcy model (2.3)–(2.8) is given as follows: find $(\overrightarrow{u}_S, p_S, \phi_D) \in X_S \times Q_S \times X_D$ such that

(3.1)
$$\begin{aligned} &\lambda c_S(\overrightarrow{u}_S, \overrightarrow{u}_S, \overrightarrow{v}) + a_S(\overrightarrow{u}_S, \overrightarrow{v}) + \lambda b_S(\overrightarrow{v}, p_S) - \lambda b_S(\overrightarrow{u}_S, q) + \lambda g a_D(\phi_D, \psi)\\ &+ \lambda\langle g\phi_D, \overrightarrow{v}\cdot\overrightarrow{n}_S\rangle - \lambda g\langle \overrightarrow{u}_S\cdot\overrightarrow{n}_S, \psi\rangle + \frac{\alpha\sqrt{\mathbf{d}}}{\sqrt{\operatorname{trace}(\prod)}}\langle P_\tau(\overrightarrow{u}_S + \mathbb{K}\nabla\phi_D), P_\tau\overrightarrow{v}\rangle\\ &= \lambda g(f_D, \psi)_{\Omega_D} + \lambda(\overrightarrow{f}_S, \overrightarrow{v})_{\Omega_S} + \lambda\langle gz, \overrightarrow{v}\cdot\overrightarrow{n}_S\rangle \ \forall\ (\overrightarrow{v}, q, \psi) \in X_S \times Q_S \times X_D. \end{aligned}$$

Here the bilinear forms are defined as

$$\begin{aligned} a_D(\phi_D, \psi) &= (\mathbb{K}\nabla\phi_D, \nabla\psi)_{\Omega_D},\\ a_S(\overrightarrow{u}_S, \overrightarrow{v}) &= 2(\mathbb{D}(\overrightarrow{u}_S), \mathbb{D}(\overrightarrow{v}))_{\Omega_S},\\ b_S(\overrightarrow{v}, q) &= -(\nabla\cdot\overrightarrow{v}, q)_{\Omega_S}, \end{aligned}$$

the projection onto the tangent space on Γ is defined as

$$P_\tau\overrightarrow{u} = \sum_{j=1}^{d-1}(\overrightarrow{u}\cdot\boldsymbol{\tau}_j)\boldsymbol{\tau}_j,$$

and the trilinear form is defined as

$$c_S(\overrightarrow{u}, \overrightarrow{w}, \overrightarrow{v}) = (\overrightarrow{u}\cdot\nabla\overrightarrow{w}, \overrightarrow{v})_{\Omega_S} + \frac{1}{2}((\nabla\cdot\overrightarrow{u})\overrightarrow{w}, \overrightarrow{v})_{\Omega_S} - \frac{1}{2}\langle\overrightarrow{u}\cdot\overrightarrow{w}, \overrightarrow{v}\cdot\overrightarrow{n}_S\rangle, \tag{3.2}$$

which is continuous on the space triplet $X_S \times X_S \times X_S$. Furthermore,

$$\begin{aligned} c_S(\overrightarrow{u}, \overrightarrow{u}, \overrightarrow{v}) &= (\overrightarrow{u}\cdot\nabla\overrightarrow{u}, \overrightarrow{v})_{\Omega_S} + \frac{1}{2}((\nabla\cdot\overrightarrow{u})\overrightarrow{u}, \overrightarrow{v})_{\Omega_S} - \frac{1}{2}\langle\overrightarrow{u}\cdot\overrightarrow{u}, \overrightarrow{v}\cdot\overrightarrow{n}_S\rangle\\ &= \frac{1}{2}(\overrightarrow{u}\cdot\nabla\overrightarrow{u}, \overrightarrow{v})_{\Omega_S} - \frac{1}{2}(\overrightarrow{u}\cdot\nabla\overrightarrow{v}, \overrightarrow{u})_{\Omega_S}\\ &\quad + \frac{1}{2}\langle\overrightarrow{u}\cdot\overrightarrow{v}, \overrightarrow{u}\cdot\overrightarrow{n}_S\rangle - \frac{1}{2}\langle\overrightarrow{u}\cdot\overrightarrow{u}, \overrightarrow{v}\cdot\overrightarrow{n}_S\rangle \ \forall\overrightarrow{u}, \overrightarrow{v} \in X_S \end{aligned} \tag{3.3}$$

since $\frac{1}{2}((\nabla\cdot\overrightarrow{u})\overrightarrow{u}, \overrightarrow{v})_{\Omega_S} = 0$. Thus, the trilinear term is completely consist with the present problem (2.3)–(2.8). Obviously, the trilinear term $c_S(\overrightarrow{u}, \overrightarrow{w}, \overrightarrow{v})$ satisfies the following identity:

$$c_S(\overrightarrow{u}, \overrightarrow{u}, \overrightarrow{u}) = 0 \ \forall\overrightarrow{u} \in X_S. \tag{3.4}$$

Remark 3.1. The space $X_S = \{\overrightarrow{v} \in [H^1(\Omega_S)]^d \mid \overrightarrow{v} = 0 \text{ on } \partial\Omega_S\backslash\Gamma\}$ is large enough to include both the solutions of the coupled weak formulation and those of the decoupled formulations in section 5. This is crucial for the analysis in this paper.

4. A branch of nonsingular solutions. In this section we will introduce a branch of the nonsingular solutions for the steady-state Navier–Stokes and Darcy equations and then utilize it to show the well-posedness of the coupled weak formulation. First, we define

$$\begin{aligned} X &= X_S \times Q_S \times X_D, \\ Y &= [H^{-1}(\Omega_S)]^d \times H^{-1}(\Omega_D), \\ V_S &= \{\overrightarrow{v} \in [H^1(\Omega_S)]^d \mid \nabla \cdot \overrightarrow{v} = 0 \text{ in } \Omega_S\} \end{aligned}$$

and

$$\begin{aligned} B((\overrightarrow{u}_S, \phi_D); (\overrightarrow{v}, \psi)) &= a_S(\overrightarrow{u}_S, \overrightarrow{v}) + \lambda g a_D(\phi_D, \psi) \\ &\quad + \lambda g \langle \phi_D, \overrightarrow{v} \cdot \overrightarrow{n}_S \rangle - \lambda g \langle \overrightarrow{u}_S \cdot \overrightarrow{n}_S, \psi \rangle \\ &\quad + \frac{\alpha \sqrt{\mathbf{d}}}{\sqrt{\operatorname{trace}(\prod)}} \langle P_\tau(\overrightarrow{u}_S + \mathbb{K}\nabla\phi_D), P_\tau \overrightarrow{v} \rangle, \end{aligned} \tag{4.1}$$

$$(F, (\overrightarrow{v}, \psi)) = (\overrightarrow{f}_S, \overrightarrow{v})_{\Omega_S} + g(f_D, \psi)_{\Omega_D} + \langle gz, \overrightarrow{v} \cdot \overrightarrow{n}_S \rangle, \tag{4.2}$$

$$(C(\overrightarrow{u}, \overrightarrow{u}), \overrightarrow{v}) = c_S(\overrightarrow{u}, \overrightarrow{u}, \overrightarrow{v}). \tag{4.3}$$

Pick $(\overrightarrow{v}, \psi) = (\overrightarrow{u}_S, \phi_D)$ in the definition of $B((\overrightarrow{u}_S, \phi_D); (\overrightarrow{v}, \psi))$; we obtain

$$\begin{aligned} B((\overrightarrow{u}_S, \phi_D); (\overrightarrow{u}_S, \phi_D)) &= a_S(\overrightarrow{u}_S, \overrightarrow{u}_S) + \lambda g a_D(\phi_D, \phi_D) \\ &\quad + \frac{\alpha \sqrt{\mathbf{d}}}{\sqrt{\operatorname{trace}(\prod)}} \langle P_\tau(\overrightarrow{u}_S + \mathbb{K}\nabla\phi_D), P_\tau \overrightarrow{u}_S \rangle. \end{aligned} \tag{4.4}$$

Consider

$$\mathbb{K} = K\mathbb{I} = \begin{pmatrix} K & 0 \\ 0 & K \end{pmatrix}.$$

By the coercivity in Lemma 3.2 of [19], when α is small enough, we have

$$B((\overrightarrow{u}_S, \phi_D); (\overrightarrow{u}_S, \phi_D)) \geq \tilde{C}_1(\|\overrightarrow{u}_S\|_1^2 + \|\phi_D\|_1^2), \tag{4.5}$$

where $\tilde{C}_1$ depends on K linearly. Hence, we have

$$B((\overrightarrow{u}_S, \phi_D); (\overrightarrow{u}_S, \phi_D)) \geq C_1 \left[a_S(\overrightarrow{u}_S, \overrightarrow{u}_S) + \lambda g a_D(\phi_D, \phi_D) \right], \tag{4.6}$$

where C_1 is independent of K.

The weak formulation (3.1) is equivalent to the following problem: given $F \in Y$, find $\bar{u}(\lambda) = (\overrightarrow{u}_S, p_S, \phi_D) \in X$ such that

$$\begin{aligned} &B((\overrightarrow{u}_S, \phi_D); (\overrightarrow{v}, \psi)) + \lambda b_S(\overrightarrow{v}, p_S) - \lambda b_S(\overrightarrow{u}_S, q) = \lambda(F, (\overrightarrow{v}, \psi)) - \lambda(C(\overrightarrow{u}_S, \overrightarrow{u}_S), \overrightarrow{v}) \\ &\forall\ (\overrightarrow{v}, q, \psi) \in X. \end{aligned} \tag{4.7}$$

Furthermore, a C^2-mapping $\mathcal{G}: R^+ \times X \to Y$ is introduced as follows:

$$\mathcal{G}(\lambda, \bar{u}(\lambda)) = \lambda \left[\begin{pmatrix} C(\overrightarrow{u}_S, \overrightarrow{u}_S) \\ 0 \end{pmatrix} - F \right]. \tag{4.8}$$

Then we define a linear operator $T \in L(Y;X)$ such that the above equation (4.7) is denoted by

$$\bar{u}(\lambda) = -T\mathcal{G}(\lambda, \bar{u}(\lambda)). \tag{4.9}$$

Then, the system (4.7) (or (3.1)) can be presented as follows:

$$\mathcal{F}(\lambda, \bar{u}(\lambda)) \equiv \bar{u}(\lambda) + T\mathcal{G}(\lambda, \bar{u}(\lambda)) = 0. \tag{4.10}$$

That is, $\bar{u}(\lambda) = (\overrightarrow{u}_S, p_S, \phi_D)$ is a solution of the problem (4.10) if and only if it is a solution of (4.7) (or (3.1)). Furthermore, $\{\lambda, \bar{u}(\lambda)\}$ is called a branch of nonsingular solutions if $D_{\bar{u}}\mathcal{G}(\lambda, \bar{u}(\lambda))$ is an isomorphism between X and Y for all $\lambda \in R^+$ [55]. Then for the branch of nonsingular solutions $\{\lambda, \bar{u}(\lambda)\}$, given any $\bar{w}_1 = (\overrightarrow{w}_1, r_1, \chi_1) \in X$, there exists a unique $\bar{w} = (\overrightarrow{w}, r, \chi) \in X$ satisfying

$$D_{\bar{u}}\mathcal{F}(\lambda, \bar{u}(\lambda))\bar{w} = \bar{w}_1. \tag{4.11}$$

Plugging (4.10) into (4.11), we obtain

$$\bar{w} - \bar{w}_1 = -TD_{\bar{u}}\mathcal{G}(\lambda, \bar{u}(\lambda))\bar{w}. \tag{4.12}$$

Using the definition of linear operator $T \in L(Y;X)$ and

$$D_{\bar{u}}\mathcal{G}(\lambda, \bar{u}(\lambda))\bar{w} = \lambda \begin{pmatrix} C(\overrightarrow{u}_S, \overrightarrow{w}) + C(\overrightarrow{w}, \overrightarrow{u}_S) \\ 0 \end{pmatrix},$$

we can obtain the following equation:

$$\begin{aligned} &B((\overrightarrow{w} - \overrightarrow{w}_1, \chi - \chi_1); (\overrightarrow{v}, \psi)) + \lambda b_S(\overrightarrow{v}, r - r_1) - \lambda b_S(\overrightarrow{w} - \overrightarrow{w}_1, q) \\ &\quad = -\lambda c_S(\overrightarrow{u}_S, \overrightarrow{w}, \overrightarrow{v}) - \lambda c_S(\overrightarrow{w}, \overrightarrow{u}_S, \overrightarrow{v}) \ \forall\ (\overrightarrow{v}, q, \psi) \in X. \end{aligned} \tag{4.13}$$

Define

$$\lambda(\tilde{f}, (\overrightarrow{v}, \psi, q)) = B((\overrightarrow{w}_1, \chi_1); (\overrightarrow{v}, \psi)) + \lambda b_S(\overrightarrow{v}, r_1) - \lambda b_S(\overrightarrow{w}_1, q) \tag{4.14}$$

and

$$\begin{aligned} B_\lambda((\overrightarrow{w}, r, \chi); (\overrightarrow{v}, q, \psi)) &= B((\overrightarrow{w}, \chi); (\overrightarrow{v}, \psi)) + \lambda b_S(\overrightarrow{v}, r) - \lambda b_S(\overrightarrow{w}, q) \\ &\quad + \lambda c_S(\overrightarrow{u}_S, \overrightarrow{w}, \overrightarrow{v}) + \lambda c_S(\overrightarrow{w}, \overrightarrow{u}_S, \overrightarrow{v}). \end{aligned} \tag{4.15}$$

Then (4.13) can be rewritten as

$$B_\lambda((\overrightarrow{w}, r, \chi); (\overrightarrow{v}, q, \psi)) = \lambda(\tilde{f}, (\overrightarrow{v}, \psi, q)) \ \forall\ (\overrightarrow{v}, q, \psi) \in X. \tag{4.16}$$

On the other hand, $D_{\bar{u}}\mathcal{G}(\lambda, \bar{u}(\lambda))$ is an injective mapping from X onto Y for each $\lambda \in R^+$. Then there exists a positive constant $\eta_0 > 0$ such that

$$||D_{\bar{u}}\mathcal{G}(\lambda, \bar{u}(\lambda))\overrightarrow{w}||_Y \geq \eta_0 \|\overrightarrow{w}\|_1 \quad \forall \overrightarrow{w} \in X_S, \tag{4.17}$$

where $||D_{\bar{u}}\mathcal{G}(\lambda, \bar{u}(\lambda))\overrightarrow{w}||_Z = \sup_{v \in X_S} \langle D_{\bar{u}}\mathcal{G}(\lambda, \bar{u}(\lambda))\overrightarrow{w}, \overrightarrow{v}\rangle / \|\overrightarrow{v}\|_1$. Then we can obtain

$$c_S(\overrightarrow{u}_S, \overrightarrow{w}, \overrightarrow{v}) + c_S(\overrightarrow{w}, \overrightarrow{u}_S, \overrightarrow{v}) \geq \frac{\eta_0}{\lambda}\|\overrightarrow{w}\|_1 \|\overrightarrow{v}\|_1 \quad \forall \overrightarrow{w},\ \overrightarrow{v} \in X_S. \tag{4.18}$$

Combining (4.6), (4.15), and (4.18), we have

$$\begin{aligned} B_\lambda((\overrightarrow{w}, r, \chi); (\overrightarrow{w}, r, \chi)) &= B((\overrightarrow{w}, \chi); (\overrightarrow{w}, \chi)) + \lambda c_S(\overrightarrow{u}_S, \overrightarrow{w}, \overrightarrow{w}) + \lambda c_S(\overrightarrow{w}, \overrightarrow{u}_S, \overrightarrow{w}) \\ &\geq B((\overrightarrow{w}, \chi); (\overrightarrow{w}, \chi)) + \eta_0 \|\overrightarrow{w}\|_1^2 \\ &\geq B((\overrightarrow{w}, \chi); (\overrightarrow{w}, \chi)) \\ &\geq C_1 \left[a_S(\overrightarrow{u}_S, \overrightarrow{u}_S) + \lambda g a_D(\phi_D, \phi_D)\right]. \end{aligned} \tag{4.19}$$

Following [12, 55, 64, 76, 77], we can obtain the next proposition based on the Lax–Milgram theory, (4.6), and (4.16) for the well-posedness of the coupled weak formulation.

PROPOSITION 4.1. *$\{\lambda, \bar{u}(\lambda)\}$ is a branch of nonsingular solutions to* (4.7) *(or* (3.1)*) if and only if there holds*

$$\begin{aligned} &B_\lambda((\overrightarrow{w}, r, \chi); (\overrightarrow{w}, r, \chi)) \geq C_1 \left[a_S(\overrightarrow{u}_S, \overrightarrow{u}_S) + \lambda g a_D(\phi_D, \phi_D)\right] \\ &\quad \forall \overrightarrow{w} \in X_S,\ r \in Q_S,\ \chi \in X_D, \end{aligned} \tag{4.20}$$

where the positive constant C_1 is independent of K.

5. Multiphysics domain decomposition method. In this section, we will propose the multiphysics DDM for solving the Naiver–Stokes–Darcy model with BJ condition.

First, in order to decouple the two physics, the components in the three interface conditions are directly reorganized to construct the Robin–Robin conditions on the interface as follows [16]:

$$\gamma_D \mathbb{K} \nabla \widehat{\phi}_D \cdot \overrightarrow{n}_D + g \widehat{\phi}_D = \eta_D \quad \text{on } \Gamma, \tag{5.1}$$

$$\overrightarrow{n}_S \cdot (\mathbb{T}(\widehat{\overrightarrow{u}}_S, \widehat{p}_S) \cdot \overrightarrow{n}_S) - \frac{1}{2} \widehat{\overrightarrow{u}}_S \cdot \widehat{\overrightarrow{u}}_S + \gamma_S \widehat{\overrightarrow{u}}_S \cdot \overrightarrow{n}_S = \eta_S \quad \text{on } \Gamma, \tag{5.2}$$

$$-P_\tau(\mathbb{T}(\widehat{\overrightarrow{u}}_S, \widehat{p}_S) \cdot \overrightarrow{n}_S) - \frac{\alpha \nu \sqrt{\mathbf{d}}}{\sqrt{\text{trace}(\prod)}} P_\tau \widehat{\overrightarrow{u}}_S = \overrightarrow{\eta}_{S\tau} \quad \text{on } \Gamma. \tag{5.3}$$

Here η_D, η_S, and $\overrightarrow{\eta}_{S\tau}$ are given functions defined on Γ. $\gamma_D > 0$ and $\gamma_S > 0$ are two positive relaxation parameters which are important to the convergence of the iteration of the proposed DDM. These two parameters are specifically designed to deal with the different velocity scales of the Stokes flow and Darcy flow, which need to match each other on the interface in the normal direction due to the interface condition (2.6). These Robin conditions are different from those conditions proposed in [34, 35, 37, 38, 39], and we consider the BJ interface condition instead of the Beavers–Joseph–Saffman interface condition or its simplification.

Then the corresponding weak formulation is given as follows: for $\eta_D \in L^2(\Gamma)$ and $\eta_S \in L^2(\Gamma)$ and $\overrightarrow{\eta}_{S\tau} \in L^2(\Gamma)$, find $\widehat{\phi}_D \in X_D$, $\widehat{\overrightarrow{u}}_S \in X_S$, and $\widehat{p}_S \in Q_S$ such that

$$a_D(\widehat{\phi}_D, \psi) + \left\langle \frac{g \widehat{\phi}_D}{\gamma_D}, \psi \right\rangle = (f_D, \psi)_{\Omega_D} + \left\langle \frac{\eta_D}{\gamma_D}, \psi \right\rangle \quad \forall\, \psi \in X_D, \tag{5.4}$$

$$\begin{aligned} &\lambda c_S(\widehat{\overrightarrow{u}}_S, \widehat{\overrightarrow{u}}_S, \overrightarrow{v})_{\Omega_S} + a_S(\widehat{\overrightarrow{u}}_S, \overrightarrow{v}) + \lambda b_S(\overrightarrow{v}, \widehat{p}_S) - \lambda b_S(\widehat{\overrightarrow{u}}_S, q) \\ &+ \lambda \gamma_S \langle \widehat{\overrightarrow{u}}_S \cdot \overrightarrow{n}_S, \overrightarrow{v} \cdot \overrightarrow{n}_S \rangle + \frac{\alpha \sqrt{\mathbf{d}}}{\sqrt{\text{trace}(\prod)}} \langle P_\tau \widehat{\overrightarrow{u}}_S, P_\tau \overrightarrow{v} \rangle \\ &\quad = \lambda(\overrightarrow{f}_S, \overrightarrow{v})_{\Omega_S} + \lambda \langle \eta_S, \overrightarrow{v} \cdot \overrightarrow{n}_S \rangle - \lambda \langle \overrightarrow{\eta}_{S\tau}, P_\tau \overrightarrow{v} \rangle \quad \forall\, (\overrightarrow{v}, q) \in X_S \times Q_S. \end{aligned} \tag{5.5}$$

One advantage of the Robin conditions proposed above is the straightforward derivation of the following compatibility conditions for the equivalence between the solutions of the Navier–Stokes–Darcy system and those of the decoupled system. Similarly to Lemma 1 in [16], we can obtain the following lemma.

LEMMA 5.1. *Let* $(\overrightarrow{u}_S, \lambda p_S, \phi_D)$ *be the solution of the coupled Navier–Stokes–Darcy system* (3.1)*, and let* $(\widehat{\overrightarrow{u}}_S, \lambda\widehat{p}_S, \widehat{\phi}_D)$ *be a branch of nonsingular solutions of the decoupled Navier–Stokes and Darcy equations* (5.4)–(5.5)*. Then,* $(\widehat{\overrightarrow{u}}_S, \lambda\widehat{p}_S, \widehat{\phi}_D) = (\overrightarrow{u}_S, \lambda p_S, \phi_D)$ *if and only if* γ_S*,* γ_D*,* η_S*,* $\overrightarrow{\eta}_{S\tau}$*, and* η_D *satisfy the following compatibility conditions:*

$$\eta_D = \gamma_D \widehat{\overrightarrow{u}}_S \cdot \overrightarrow{n}_S + g\widehat{\phi}_D, \tag{5.6}$$

$$\eta_S = \gamma_S \widehat{\overrightarrow{u}}_S \cdot \overrightarrow{n}_S - g\widehat{\phi}_D + gz, \tag{5.7}$$

$$\overrightarrow{\eta}_{S\tau} = \frac{\alpha\nu\sqrt{\boldsymbol{d}}}{\sqrt{\mathrm{trace}(\prod)}} P_\tau(\mathbb{K}\nabla\widehat{\phi}_D). \tag{5.8}$$

These compatibility conditions provide convenient tools to directly predict ξ_D, ξ_S and $\xi_{S\tau}$ on the interface at each time step based on the results from the previous time steps. Hence we can propose a multi-physics DDM as follows.

1. Initial values η_D^0, η_S^0 and $\overrightarrow{\eta}_{S\tau}^0$ are guessed. They may be taken to be zero.
2. For $k = 0, 1, 2, \ldots$, independently solve the Darcy and Navier–Stokes equationss with the Robin boundary conditions on the interface, which are constructed in section 5. More precisely, $\phi_D^k \in X_D$ is computed from

$$a_D(\phi_D^k, \psi) + \langle \frac{g\phi_D^k}{\gamma_D}, \psi\rangle = \langle \frac{\eta_D^k}{\gamma_D}, \psi\rangle + (f_D, \psi)_{\Omega_D}, \qquad \forall\, \psi \in X_D, \tag{5.9}$$

and $(\overrightarrow{u}_S^k, p_S^k) \in X_S \times Q_S$ are computed from:

$$\begin{aligned} &\lambda c_S(\overrightarrow{u}_S^k, \overrightarrow{u}_S^k, \overrightarrow{v})_{\Omega_S} + a_S(\overrightarrow{u}_S^k, \overrightarrow{v}) + \lambda b_S(\overrightarrow{v}, p_S^k) - \lambda b_S(\overrightarrow{u}_S^k, q) \\ &+\lambda\gamma_S\langle \overrightarrow{u}_S^k \cdot \overrightarrow{n}_S, \overrightarrow{v} \cdot \overrightarrow{n}_S\rangle + \frac{\alpha\sqrt{\mathbf{d}}}{\sqrt{\mathrm{trace}(\prod)}}\langle P_\tau \overrightarrow{u}_S^k, P_\tau \overrightarrow{v}\rangle \\ &= \lambda(\overrightarrow{f}_S, \overrightarrow{v})_{\Omega_S} + \lambda\langle \eta_S^k, \overrightarrow{v} \cdot \overrightarrow{n}_S\rangle - \lambda\langle \overrightarrow{\eta}_{S\tau}^k, P_\tau \overrightarrow{v}\rangle, \quad (\overrightarrow{v}, q) \in X_S \times Q_S. \end{aligned} \tag{5.10}$$

3. η_D^{k+1}, η_S^{k+1} and $\overrightarrow{\eta}_{S\tau}^{k+1}$ are updated in the following manner:

$$\eta_S^{k+1} = \frac{\gamma_S}{\gamma_D}\eta_D^k - (1 + \frac{\gamma_S}{\gamma_D})g\phi_D^k + gz, \tag{5.11}$$

$$\eta_D^{k+1} = -\eta_S^k + (\gamma_S + \gamma_D)\overrightarrow{u}_S^k \cdot \overrightarrow{n}_S + gz, \tag{5.12}$$

$$\overrightarrow{\eta}_{S\tau}^{k+1} = \frac{\alpha\nu\sqrt{\mathbf{d}}}{\sqrt{\mathrm{trace}(\prod)}} P_\tau(\mathbb{K}\nabla\phi_D^k), \tag{5.13}$$

6. Convergence of the domain decomposition method. In this section we will follow the elegant energy method proposed in [79] and the arguments in [16] to demonstrate the convergence of the proposed DDM for appropriate choice of parameters γ_D and γ_S. The new, major difficulty is the extension of the previous analysis for the nonlinear advection in the Navier–Stokes equations.

Let $(\overrightarrow{u}_S, p_S, \phi_D)$ denote the solution of the coupled Stokes–Darcy system (3.1) for a given $\lambda \in R^+$. Then we have that $(\overrightarrow{u}_S, p_S, \phi_D)$ solves the equivalent decoupled system (5.4)–(5.5) with γ_S, γ_D, η_D, η_S, and $\overrightarrow{\eta}_{S\tau}$ satisfying the compatibility conditions (5.6)–(5.8) with the hats removed. Next, we define the error functions

$$\begin{aligned} &\varepsilon_D^k = \eta_D - \eta_D^k, \quad \varepsilon_S^k = \eta_S - \eta_S^k, \qquad \overrightarrow{\varepsilon}_{S\tau}^k = \overrightarrow{\eta}_{S\tau} - \overrightarrow{\eta}_{S\tau}^k, \\ &e_\phi^k = \phi_D - \phi_D^k, \quad \overrightarrow{e}_u^k = \overrightarrow{u}_S - \overrightarrow{u}_S^k, \qquad e_p^k = p_S - p_S^k, \end{aligned}$$

and then provide the error equations in the following two lemmas.

LEMMA 6.1. *The error functions satisfy*

$$\begin{aligned} \lambda\|\varepsilon_D^{k+1}\|_\Gamma^2 = \lambda\|\varepsilon_S^k\|_\Gamma^2 - 2(\gamma_S+\gamma_D)\Big[&\lambda c_S(\overrightarrow{e}_u^k, \overrightarrow{u}_S, \overrightarrow{e}_u^k) \\ &+ \lambda c_S(\overrightarrow{u}_S, \overrightarrow{e}_u^k, \overrightarrow{e}_u^k) + a_S(\overrightarrow{e}_u^k, \overrightarrow{e}_u^k) \\ &+ \frac{\alpha\sqrt{\boldsymbol{d}}}{\sqrt{\operatorname{trace}(\prod)}}\langle P_\tau(\overrightarrow{e}_u^k + \mathbb{K}\nabla e_\phi^{k-1}), P_\tau\overrightarrow{e}_u^k\rangle\Big] \\ &+ \lambda(\gamma_D^2 - \gamma_S^2)\|\overrightarrow{e}_u^k\cdot\overrightarrow{n}_S\|_\Gamma^2. \end{aligned} \tag{6.1}$$

Proof. First, we analyze the errors from trilinear terms:

$$\begin{aligned} &c_S(\overrightarrow{u}_S, \overrightarrow{u}_S, \overrightarrow{v}) - c_S(\overrightarrow{u}_S^k, \overrightarrow{u}_S^k, \overrightarrow{v}) \\ &\quad = c_S(\overrightarrow{u}_S, \overrightarrow{u}_S, \overrightarrow{v}) - c_S(\overrightarrow{u}_S^k, \overrightarrow{u}_S, \overrightarrow{v}) + c_S(\overrightarrow{u}_S^k, \overrightarrow{u}_S, \overrightarrow{v}) - c_S(\overrightarrow{u}_S^k, \overrightarrow{u}_S^k, \overrightarrow{v}) \\ &\quad = c_S(\overrightarrow{e}_u^k, \overrightarrow{u}_S, \overrightarrow{v}) + c_S(\overrightarrow{u}_S^k, \overrightarrow{e}_u^k, \overrightarrow{v}) \\ &\quad = c_S(\overrightarrow{e}_u^k, \overrightarrow{u}_S, \overrightarrow{v}) + c_S(\overrightarrow{u}_S, \overrightarrow{e}_u^k, \overrightarrow{v}) - c_S(\overrightarrow{u}_S, \overrightarrow{e}_u^k, \overrightarrow{v}) + c_S(\overrightarrow{u}_S^k, \overrightarrow{e}_u^k, \overrightarrow{v}) \\ &\quad = c_S(\overrightarrow{e}_u^k, \overrightarrow{u}_S, \overrightarrow{v}) + c_S(\overrightarrow{u}_S, \overrightarrow{e}_u^k, \overrightarrow{v}) - c_S(\overrightarrow{e}_u^k, \overrightarrow{e}_u^k, \overrightarrow{v}). \end{aligned} \tag{6.2}$$

Subtracting (5.5) from (5.10) and applying (6.2), we obtain

$$\begin{aligned} &\lambda c_S(\overrightarrow{e}_u^k, \overrightarrow{u}_S, \overrightarrow{v}) + \lambda c_S(\overrightarrow{u}_S, \overrightarrow{e}_u^k, \overrightarrow{v}) - \lambda c_S(\overrightarrow{e}_u^k, \overrightarrow{e}_u^k, \overrightarrow{v}) \\ &\quad + a_S(\overrightarrow{e}_u^k, \overrightarrow{v}) + \lambda b_S(\overrightarrow{v}, e_p^k) - \lambda b_S(\overrightarrow{e}_u^k, q) + \lambda\gamma_S\langle\overrightarrow{e}_u^k\cdot\overrightarrow{n}_S, \overrightarrow{v}\cdot\overrightarrow{n}_S\rangle \\ &\quad + \frac{\alpha\sqrt{\mathbf{d}}}{\sqrt{\operatorname{trace}(\prod)}}\langle P_\tau\overrightarrow{e}_u^k, P_\tau\overrightarrow{v}\rangle \\ &= \lambda\langle\varepsilon_S^k, \overrightarrow{v}\cdot\overrightarrow{n}_S\rangle - \lambda\langle\overrightarrow{\varepsilon}_{S\tau}^k, P_\tau\overrightarrow{v}\rangle \quad \forall\,(\overrightarrow{v}, q) \in X_S \times Q_S. \end{aligned} \tag{6.3}$$

Note that $\overrightarrow{u}_S, \overrightarrow{u}_S^k \in X_S$. Then $\overrightarrow{e}_u^k \in X_S$ and (3.4) lead to

$$c_S(\overrightarrow{e}_u^k, \overrightarrow{e}_u^k, \overrightarrow{e}_u^k) = 0. \tag{6.4}$$

Setting $(\overrightarrow{v}, q) = (\overrightarrow{e}_u^k, e_p^k)$ in (6.3), we get

$$\begin{aligned} \lambda c_S(\overrightarrow{e}_u^k, \overrightarrow{u}_S, \overrightarrow{e}_u^k) + \lambda c_S(\overrightarrow{u}_S, \overrightarrow{e}_u^k, \overrightarrow{e}_u^k) + a_S(\overrightarrow{e}_u^k, \overrightarrow{e}_u^k) \\ + \lambda\gamma_S\|\overrightarrow{e}_u^k\cdot\overrightarrow{n}_S\|_\Gamma^2 + \frac{\alpha\sqrt{\mathbf{d}}}{\sqrt{\operatorname{trace}(\prod)}}\langle P_\tau\overrightarrow{e}_u^k, P_\tau\overrightarrow{e}_u^k\rangle \\ = \lambda\langle\varepsilon_S^k, \overrightarrow{e}_u^k\cdot\overrightarrow{n}_S\rangle - \lambda\langle\overrightarrow{\varepsilon}_{S\tau}^k, P_\tau\overrightarrow{e}_u^k\rangle. \end{aligned} \tag{6.5}$$

Along the interface Γ, the errors satisfy

$$\overrightarrow{\varepsilon}_{S\tau}^{k+1} = \frac{\alpha\nu\sqrt{\mathbf{d}}}{\sqrt{\mathrm{trace}(\prod)}} P_\tau(\mathbb{K}\nabla e_\phi^k). \tag{6.6}$$

By (6.5) and (6.6), we have

$$\begin{aligned}\lambda\langle \varepsilon_S^k, \overrightarrow{e}_u^k \cdot \overrightarrow{n}_S\rangle &= \lambda c_S(\overrightarrow{e}_u^k, \overrightarrow{u}_S, \overrightarrow{v}) + \lambda c_S(\overrightarrow{u}_S, \overrightarrow{e}_u^k, \overrightarrow{v}) + a_S(\overrightarrow{e}_u^k, \overrightarrow{e}_u^k)\\ &\quad + \frac{\alpha\sqrt{\mathbf{d}}}{\sqrt{\mathrm{trace}(\prod)}}\langle P_\tau(\overrightarrow{e}_u^k + \mathbb{K}\nabla e_\phi^{k-1}), P_\tau \overrightarrow{e}_u^k\rangle + \lambda\gamma_S \|\overrightarrow{e}_u^k \cdot \overrightarrow{n}_S\|_\Gamma^2.\end{aligned} \tag{6.7}$$

Furthermore, we have

$$\varepsilon_D^{k+1} = -\varepsilon_S^k + (\gamma_S + \gamma_D)\overrightarrow{e}_u^k \cdot \overrightarrow{n}_S, \tag{6.8}$$

which leads to

$$\|\varepsilon_D^{k+1}\|_\Gamma^2 = \|\varepsilon_S^k\|_\Gamma^2 + (\gamma_S+\gamma_D)^2\|\overrightarrow{e}_u^k \cdot \overrightarrow{n}_S\|_\Gamma^2 - 2(\gamma_S+\gamma_D)\langle \varepsilon_S^k, \overrightarrow{e}_u^k \cdot \overrightarrow{n}_S\rangle. \tag{6.9}$$

Plugging (6.7) into (6.9), we obtain

$$\begin{aligned}\lambda\|\varepsilon_D^{k+1}\|_\Gamma^2 &= \lambda\|\varepsilon_S^k\|_\Gamma^2 + \lambda\left[(\gamma_S+\gamma_D)^2 - 2(\gamma_S+\gamma_D)\gamma_S\right]\|\overrightarrow{e}_u^k \cdot \overrightarrow{n}_S\|_\Gamma^2\\ &\quad - 2(\gamma_S+\gamma_D)\left[\lambda c_S(\overrightarrow{e}_u^k, \overrightarrow{u}_S^k, \overrightarrow{v}) + \lambda c_S(\overrightarrow{u}_S^k, \overrightarrow{e}_u^k, \overrightarrow{v}) + a_S(\overrightarrow{e}_u^k, \overrightarrow{e}_u^k)\right.\\ &\quad \left. + \frac{\alpha\sqrt{\mathbf{d}}}{\sqrt{\mathrm{trace}(\prod)}}\langle P_\tau(\overrightarrow{e}_u^k + \mathbb{K}\nabla e_\phi^{k-1}), P_\tau \overrightarrow{e}_u^k\rangle\right],\end{aligned} \tag{6.10}$$

which completes the proof of (6.1). ∎

Furthermore, we recall the following conclusion from [16].

LEMMA 6.2. *The error functions satisfy*

$$\|\varepsilon_S^{k+1}\|_\Gamma^2 = \left(\frac{\gamma_S}{\gamma_D}\right)^2\|\varepsilon_D^k\|_\Gamma^2 + \left[1 - \left(\frac{\gamma_S}{\gamma_D}\right)^2\right]\|g e_\phi^k\|_\Gamma^2 - 2\gamma_S\left(1 + \frac{\gamma_S}{\gamma_D}\right) g\, a_D(e_\phi^k, e_\phi^k). \tag{6.11}$$

In the rest of this section, we will carry out the convergence analysis for $\gamma_S = \gamma_D$ and $\gamma_S < \gamma_D$ in Theorem 6.3 and Theorem 6.4 separately.

THEOREM 6.3. *Under the assumption of Proposition* 4.1*, if* $\gamma_S = \gamma_D = \gamma > 0$*,* $\mathbb{K}$ *is isotropic, and* α *is small enough such that* (6.15) *and* (6.19) *are satisfied, then the domain decomposition solution* $(\overrightarrow{u}_S^k, p_S^k, \phi_D^k)$ *converges to the analytic solution* $(\overrightarrow{u}_S, p_S, \phi_D)$*.*

Proof. From Lemma 6.1, Lemma 6.2, and $\gamma_S = \gamma_D = \gamma$, we have

$$\begin{aligned}\lambda\|\varepsilon_D^{k+1}\|_\Gamma^2 &= \lambda\|\varepsilon_S^k\|_\Gamma^2 - 4\gamma\left[\lambda c_S(\overrightarrow{e}_u^k, \overrightarrow{u}_S, \overrightarrow{e}_u^k) + \lambda c_S(\overrightarrow{u}_S, \overrightarrow{e}_u^k, \overrightarrow{e}_u^k) + a_S(\overrightarrow{e}_u^k, \overrightarrow{e}_u^k)\right.\\ &\quad \left. + \frac{\alpha\sqrt{\mathbf{d}}}{\sqrt{\mathrm{trace}(\prod)}}\langle P_\tau(\overrightarrow{e}_u^k + \mathbb{K}\nabla e_\phi^{k-1}), P_\tau \overrightarrow{e}_u^k\rangle\right],\end{aligned} \tag{6.12}$$

$$\lambda\|\varepsilon_S^{k+1}\|_\Gamma^2 = \lambda\|\varepsilon_D^k\|_\Gamma^2 - 4\lambda\gamma g a_D(e_\phi^k, e_\phi^k). \tag{6.13}$$

Adding the two equations and summing over k from $k=1$ to N, we obtain

$$\begin{aligned} 0 \le\ & \lambda\|\varepsilon_D^{N+1}\|_\Gamma^2 + \lambda\|\varepsilon_S^{N+1}\|_\Gamma^2 \\ =\ & \lambda\|\varepsilon_D^1\|_\Gamma^2 + \lambda\|\varepsilon_S^1\|_\Gamma^2 - 4\gamma\sum_{k=1}^N \Bigg[\lambda c_S(\overrightarrow{e}_u^k, \overrightarrow{u}_S, \overrightarrow{e}_u^k) + \lambda c_S(\overrightarrow{u}_S, \overrightarrow{e}_u^k, \overrightarrow{e}_u^k) \\ & + a_S(\overrightarrow{e}_u^k, \overrightarrow{e}_u^k) + \lambda g\ a_D(e_\phi^k, e_\phi^k) + \frac{\alpha\sqrt{\mathbf{d}}}{\sqrt{\mathrm{trace}(\prod)}}\langle P_\tau(\overrightarrow{e}_u^k + \mathbb{K}\nabla e_\phi^k), P_\tau\overrightarrow{e}_u^k\rangle\Bigg] \\ & - 4\gamma\sum_{k=1}^N \frac{\alpha\sqrt{\mathbf{d}}}{\sqrt{\mathrm{trace}(\prod)}}\langle P_\tau(\mathbb{K}\nabla e_\phi^{k-1} - \mathbb{K}\nabla e_\phi^k), P_\tau\overrightarrow{e}_u^k\rangle. \end{aligned} \tag{6.14}$$

By Proposition 4.1, when α is small enough, we have

$$\begin{aligned} & \lambda c_S(\overrightarrow{e}_u^k, \overrightarrow{u}_S, \overrightarrow{e}_u^k) + \lambda c_S(\overrightarrow{u}_S, \overrightarrow{e}_u^k, \overrightarrow{e}_u^k) + a_S(\overrightarrow{e}_u^k, \overrightarrow{e}_u^k) + \lambda g\ a_D(e_\phi^k, e_\phi^k) \\ & + \frac{\alpha\sqrt{\mathbf{d}}}{\sqrt{\mathrm{trace}(\prod)}}\langle P_\tau(\overrightarrow{e}_u^k + \mathbb{K}\nabla e_\phi^k), P_\tau\overrightarrow{e}_u^k\rangle \\ & \ge\ C_1\left[a_S(\overrightarrow{e}_u^k, \overrightarrow{e}_u^k) + \lambda g a_D(e_\phi^k, e_\phi^k)\right]. \end{aligned} \tag{6.15}$$

Since we suppose $\mathbb{K}$ is isotropic, $\mathbb{K} = K\mathbb{I}$, where K is an constant and $\mathbb{I}$ is the identity matrix. Based on (5.36) in [16], we have

$$\sum_{k=1}^N \langle P_\tau(\mathbb{K}\nabla e_\phi^{k-1} - \mathbb{K}\nabla e_\phi^k), P_\tau\overrightarrow{e}_u^k\rangle \ \ge\ -\tilde{C}_2\sum_{k=0}^N\left(\|\overrightarrow{e}_u^k\|_1^2 + \|e_\phi^k\|_1^2\right), \tag{6.16}$$

where $\tilde{C}_2$ depends on K linearly. Hence,

$$\sum_{k=1}^N \langle P_\tau(\mathbb{K}\nabla e_\phi^{k-1} - \mathbb{K}\nabla e_\phi^k), P_\tau\overrightarrow{e}_u^k\rangle \ge -C_2\sum_{k=0}^N\left[a_S(\overrightarrow{e}_u^k, \overrightarrow{e}_u^k) + \lambda g a_D(e_\phi^k, e_\phi^k)\right], \tag{6.17}$$

where C_2 is also independent of K.

Then plugging (6.15) and (6.17) into (6.14), we get

$$\begin{aligned} & 4\gamma\left(C_1 - C_2\frac{\alpha\sqrt{\mathbf{d}}}{\sqrt{\mathrm{trace}(\prod)}}\right)\sum_{k=0}^N\left[a_S(\overrightarrow{e}_u^k, \overrightarrow{e}_u^k) + \lambda g a_D(e_\phi^k, e_\phi^k)\right] \\ & \quad \le \left(\|\varepsilon_D^1\|_\Gamma^2 + \|\varepsilon_S^1\|_\Gamma^2\right) + 4\gamma C_1\left[a_S(\overrightarrow{e}_u^0, \overrightarrow{e}_u^0) + \lambda g a_D(e_\phi^0, e_\phi^0)\right] \end{aligned} \tag{6.18}$$

for any positive integer N. If α is small enough such that

$$C_1 - C_2\frac{\alpha\sqrt{\mathbf{d}}}{\sqrt{\mathrm{trace}(\prod)}} > 0, \tag{6.19}$$

then $\overrightarrow{e}_u^k$ and e_ϕ^k tend to zero by the convergence theorem of series of positive terms. Hence, we obtain the convergence of ϕ_D^k and $\overrightarrow{u}_S^k$ to the hydraulic head ϕ_D and the

velocity $\overrightarrow{u}_S$, respectively. The convergence of p_S^k to the pressure p_S then follows from the inf-sup condition and (6.3). ∎

Now we turn to the analysis for the case of $0 < \gamma_S < \gamma_D$. In this case, we will first show the convergence and then derive a geometric convergence rate.

THEOREM 6.4. *Under the assumption of Proposition* 4.1, *if* $0 < \gamma_S < \gamma_D$, $\mathbb{K}$ *is isotropic,* α *is small enough such that* (6.15) *and* (6.19) *are satisfied, and* γ_S *and* γ_D *are close to each other such that* (6.25) *and* (6.26) *are satisfied, then the domain decomposition solution* $(\overrightarrow{u}_S^k, p_S^k, \phi_D^k)$ *converges to the analytic solution* $(\overrightarrow{u}_S, p_S, \phi_D)$. *Furthermore, if* (6.34) *and* (6.35) *are satisfied, then we have geometric convergence rate* $\sqrt{\frac{\gamma_S}{\gamma_D}}$.

Proof. Multiplying (6.1) by $\frac{\gamma_S}{\gamma_D}$ and (6.11) by λ and adding them together, we get

(6.20)

$$
\begin{aligned}
&\lambda\frac{\gamma_S}{\gamma_D}\|\varepsilon_D^{k+1}\|_\Gamma^2 + \lambda\|\varepsilon_S^{k+1}\|_\Gamma^2 \\
&= \lambda\frac{\gamma_S}{\gamma_D}\|\varepsilon_S^k\|_\Gamma^2 - 2\frac{\gamma_S}{\gamma_D}(\gamma_S+\gamma_D)\left[\lambda c_S(\overrightarrow{e}_u^k, \overrightarrow{u}_S, \overrightarrow{e}_u^k) + \lambda c_S(\overrightarrow{u}_S, \overrightarrow{e}_u^k, \overrightarrow{e}_u^k)\right. \\
&\quad \left. + a_S(\overrightarrow{e}_u^k, \overrightarrow{e}_u^k) + \frac{\alpha\sqrt{\mathbf{d}}}{\sqrt{\operatorname{trace}(\prod)}}\langle P_\tau(\overrightarrow{e}_u^k + \mathbb{K}\nabla e_\phi^{k-1}), P_\tau\overrightarrow{e}_u^k\rangle\right] \\
&\quad + \lambda\frac{\gamma_S}{\gamma_D}(\gamma_D^2-\gamma_S^2)\|\overrightarrow{e}_u^k\cdot\overrightarrow{n}_S\|_\Gamma^2 + \lambda\left(\frac{\gamma_S}{\gamma_D}\right)^2\|\varepsilon_D^k\|_\Gamma^2 + \lambda\left[1-\left(\frac{\gamma_S}{\gamma_D}\right)^2\right]\|ge_\phi^k\|_\Gamma^2 \\
&\quad - 2\lambda\gamma_S\left(1+\frac{\gamma_S}{\gamma_D}\right)g\,a_D(e_\phi^k, e_\phi^k) = -2\frac{\gamma_S}{\gamma_D}(\gamma_S+\gamma_D)\left[\lambda c_S(\overrightarrow{e}_u^k, \overrightarrow{u}_S, \overrightarrow{e}_u^k)\right. \\
&\quad + \lambda c_S(\overrightarrow{u}_S, \overrightarrow{e}_u^k, \overrightarrow{e}_u^k) + a_S(\overrightarrow{e}_u^k, \overrightarrow{e}_u^k) + \lambda g\,a_D(e_\phi^k, e_\phi^k) \\
&\quad \left. + \frac{\alpha\sqrt{\mathbf{d}}}{\sqrt{\operatorname{trace}(\prod)}}\langle P_\tau(\overrightarrow{e}_u^k + \mathbb{K}\nabla e_\phi^k), P_\tau\overrightarrow{e}_u^k\rangle\right] \\
&\quad - 2\frac{\gamma_S}{\gamma_D}(\gamma_S+\gamma_D)\frac{\alpha\sqrt{\mathbf{d}}}{\sqrt{\operatorname{trace}(\prod)}}\langle P_\tau(\mathbb{K}\nabla e_\phi^{k-1} - \mathbb{K}\nabla e_\phi^k), P_\tau\overrightarrow{e}_u^k\rangle \\
&\quad + \lambda\frac{\gamma_S}{\gamma_D}(\gamma_D^2-\gamma_S^2)\|\overrightarrow{e}_u^k\cdot\overrightarrow{n}_S\|_\Gamma^2 + \lambda\left(1-\left(\frac{\gamma_S}{\gamma_D}\right)^2\right)\|ge_\phi^k\|_\Gamma^2 \\
&\quad + \lambda\left(\frac{\gamma_S}{\gamma_D}\right)^2\|\varepsilon_D^k\|_\Gamma^2 + \lambda\frac{\gamma_S}{\gamma_D}\|\varepsilon_S^k\|_\Gamma^2.
\end{aligned}
$$

Then summing over k from $k=1$ to N, we obtain

(6.21)

$$
0 \le \lambda\sum_{k=2}^{N}\left[\frac{\gamma_S}{\gamma_D} - (\frac{\gamma_S}{\gamma_D})^2\right]\|\varepsilon_D^k\|_\Gamma^2 + \lambda\sum_{k=2}^{N}\left[1-\frac{\gamma_S}{\gamma_D}\right]\|\varepsilon_S^k\|_\Gamma^2 + \lambda\frac{\gamma_S}{\gamma_D}\|\varepsilon_D^{N+1}\|_\Gamma^2 + \lambda\|\varepsilon_S^{N+1}\|_\Gamma^2
$$

$$
\begin{aligned}
&= -2\frac{\gamma_S}{\gamma_D}(\gamma_S+\gamma_D)\sum_{k=1}^{N}\Bigg[\lambda c_S(\overrightarrow{e}_u^k,\overrightarrow{u}_S,\overrightarrow{e}_u^k)+\lambda c_S(\overrightarrow{u}_S,\overrightarrow{e}_u^k,\overrightarrow{e}_u^k)+a_S(\overrightarrow{e}_u^k,\overrightarrow{e}_u^k)\\
&\quad+\lambda g\, a_D(e_\phi^k,e_\phi^k)+\frac{\alpha\sqrt{\mathbf{d}}}{\sqrt{\mathrm{trace}(\prod)}}\langle P_\tau(\overrightarrow{e}_u^k+\mathbb{K}\nabla e_\phi^k),P_\tau\overrightarrow{e}_u^k\rangle\Bigg]\\
&\quad-2\frac{\gamma_S}{\gamma_D}(\gamma_S+\gamma_D)\frac{\alpha\sqrt{\mathbf{d}}}{\sqrt{\mathrm{trace}(\prod)}}\sum_{k=1}^{N}\langle P_\tau(\mathbb{K}\nabla e_\phi^{k-1}-\mathbb{K}\nabla e_\phi^k),P_\tau\overrightarrow{e}_u^k\rangle\\
&\quad+\lambda\frac{\gamma_S}{\gamma_D}(\gamma_D^2-\gamma_S^2)\sum_{k=1}^{N}\|\overrightarrow{e}_u^k\cdot\overrightarrow{n}_S\|_\Gamma^2\\
&\quad+\lambda\left(1-\left(\frac{\gamma_S}{\gamma_D}\right)^2\right)\sum_{k=1}^{N}\|ge_\phi^k\|_\Gamma^2+\lambda\left(\frac{\gamma_S}{\gamma_D}\right)^2\|\varepsilon_D^1\|_\Gamma^2+\lambda\frac{\gamma_S}{\gamma_D}\|\varepsilon_S^1\|_\Gamma^2.
\end{aligned}
$$

By the trace inequality, Poincaré inequality, and Korn's inequality we have

$$\|\overrightarrow{e}_u^k\cdot\overrightarrow{n}_S\|_\Gamma^2\le C_3a_S(\overrightarrow{e}_u^k,\overrightarrow{e}_u^k), \tag{6.22}$$

$$\|ge_\phi^k\|_\Gamma^2\le g^2\frac{C_4}{K}a_D(e_\phi^k,e_\phi^k). \tag{6.23}$$

Plugging (6.15), (6.17), (6.22), and (6.23) into (6.21), we get

(6.24)

$$
\begin{aligned}
0&\le\lambda\sum_{k=2}^{N}\left[\frac{\gamma_S}{\gamma_D}-\left(\frac{\gamma_S}{\gamma_D}\right)^2\right]\|\varepsilon_D^k\|_\Gamma^2+\lambda\sum_{k=2}^{N}\left[1-\frac{\gamma_S}{\gamma_D}\right]\|\varepsilon_S^k\|_\Gamma^2+\lambda\frac{\gamma_S}{\gamma_D}\|\varepsilon_D^{N+1}\|_\Gamma^2+\lambda\|\varepsilon_S^{N+1}\|_\Gamma^2\\
&\le-2\frac{\gamma_S}{\gamma_D}(\gamma_S+\gamma_D)C_1\sum_{k=1}^{N}\left[a_S(\overrightarrow{e}_u^k,\overrightarrow{e}_u^k)+\lambda g a_D(e_\phi^k,e_\phi^k)\right]\\
&\quad+2\frac{\gamma_S}{\gamma_D}(\gamma_S+\gamma_D)\frac{\alpha\sqrt{\mathbf{d}}}{\sqrt{\mathrm{trace}(\prod)}}C_2\sum_{k=0}^{N}\left[a_S(\overrightarrow{e}_u^k,\overrightarrow{e}_u^k)+\lambda g a_D(e_\phi^k,e_\phi^k)\right]\\
&\quad+\lambda\frac{\gamma_S}{\gamma_D}(\gamma_D^2-\gamma_S^2)C_3\sum_{k=1}^{N}a_S(\overrightarrow{e}_u^k,\overrightarrow{e}_u^k)+\lambda\left(1-\left(\frac{\gamma_S}{\gamma_D}\right)^2\right)g^2\frac{C_4}{K}\sum_{k=1}^{N}a_D(e_\phi^k,e_\phi^k)\\
&\quad+\lambda\left(\frac{\gamma_S}{\gamma_D}\right)^2\|\varepsilon_D^1\|_\Gamma^2+\lambda\frac{\gamma_S}{\gamma_D}\|\varepsilon_S^1\|_\Gamma^2\\
&=-(2-s)\frac{\gamma_S}{\gamma_D}(\gamma_S+\gamma_D)\left[C_1-\frac{\alpha\sqrt{\mathbf{d}}}{\sqrt{\mathrm{trace}(\prod)}}C_2\right]\sum_{k=1}^{N}\left[a_S(\overrightarrow{e}_u^k,\overrightarrow{e}_u^k)+\lambda g a_D(e_\phi^k,e_\phi^k)\right]\\
&\quad+\left[\lambda\frac{\gamma_S}{\gamma_D}(\gamma_D^2-\gamma_S^2)C_3-s\frac{\gamma_S}{\gamma_D}(\gamma_S+\gamma_D)\left(C_1-\frac{\alpha\sqrt{\mathbf{d}}}{\sqrt{\mathrm{trace}(\prod)}}C_2\right)\right]\sum_{k=1}^{N}a_S(\overrightarrow{e}_u^k,\overrightarrow{e}_u^k)\\
&\quad+\left[\left(1-\left(\frac{\gamma_S}{\gamma_D}\right)^2\right)g\frac{C_4}{K}-s\frac{\gamma_S}{\gamma_D}(\gamma_S+\gamma_D)\left(C_1-\frac{\alpha\sqrt{\mathbf{d}}}{\sqrt{\mathrm{trace}(\prod)}}C_2\right)\right]\sum_{k=1}^{N}\lambda g a_D(e_\phi^k,e_\phi^k)\\
&\quad+\lambda\left(\frac{\gamma_S}{\gamma_D}\right)^2\|\varepsilon_D^1\|_\Gamma^2+\lambda\frac{\gamma_S}{\gamma_D}\|\varepsilon_S^1\|_\Gamma^2\\
&\quad+2\frac{\gamma_S}{\gamma_D}(\gamma_S+\gamma_D)\frac{\alpha\sqrt{\mathbf{d}}}{\sqrt{\mathrm{trace}(\prod)}}C_2\left[a_S(\overrightarrow{e}_u^0,\overrightarrow{e}_u^0)+\lambda g a_D(e_\phi^0,e_\phi^0)\right]
\end{aligned}
$$

for any $s \in (0,2)$. Suppose γ_S and γ_D are chosen such that

$$\lambda\frac{\gamma_S}{\gamma_D}(\gamma_D^2-\gamma_S^2)C_3 - s\frac{\gamma_S}{\gamma_D}(\gamma_S+\gamma_D)\left(C_1 - \frac{\alpha\sqrt{\mathbf{d}}}{\sqrt{\operatorname{trace}(\prod)}}C_2\right) \le 0, \tag{6.25}$$

$$\left(1-\left(\frac{\gamma_S}{\gamma_D}\right)^2\right) g\frac{C_4}{K} - s\frac{\gamma_S}{\gamma_D}(\gamma_S+\gamma_D)\left(C_1 - \frac{\alpha\sqrt{\mathbf{d}}}{\sqrt{\operatorname{trace}(\prod)}}C_2\right) \le 0. \tag{6.26}$$

Then we get

(6.27)

$$\begin{aligned}
&(2-s)\frac{\gamma_S}{\gamma_D}(\gamma_S+\gamma_D)\left(C_1 - \frac{\alpha\sqrt{\mathbf{d}}}{\sqrt{\operatorname{trace}(\prod)}}C_2\right)\sum_{k=1}^{N}\left[a_S(\overrightarrow{e}_u^k, \overrightarrow{e}_u^k) + \lambda g a_D(e_\phi^k, e_\phi^k)\right] \\
&\le \lambda\left(\frac{\gamma_S}{\gamma_D}\right)^2 \|\varepsilon_D^1\|_\Gamma^2 + \lambda\frac{\gamma_S}{\gamma_D}\|\varepsilon_S^1\|_\Gamma^2 \\
&\quad + 2\frac{\gamma_S}{\gamma_D}(\gamma_S+\gamma_D)\frac{\alpha\sqrt{\mathbf{d}}}{\sqrt{\operatorname{trace}(\prod)}}C_2\left[a_S(\overrightarrow{e}_u^0, \overrightarrow{e}_u^0) + \lambda g a_D(e_\phi^0, e_\phi^0)\right].
\end{aligned}$$

With the same argument as at the end of the proof of Theorem 6.3, we obtain the convergence if α is small enough such that (6.19) is true.

Now we derive a geometric convergence rate. Plugging (6.11) into (6.1), we have

$$\begin{aligned}
\lambda\|\varepsilon_D^{k+1}\|_\Gamma^2 &= -2(\gamma_S+\gamma_D)\left[\lambda c_S(\overrightarrow{e}_u^k, \overrightarrow{u}_S, \overrightarrow{e}_u^k) + \lambda c_S(\overrightarrow{u}_S, \overrightarrow{e}_u^k, \overrightarrow{e}_u^k) + a_S(\overrightarrow{e}_u^k, \overrightarrow{e}_u^k)\right. \\
&\qquad \left. + \frac{\alpha\sqrt{\mathbf{d}}}{\sqrt{\operatorname{trace}(\prod)}}\langle P_\tau(\overrightarrow{e}_u^k + \mathbb{K}\nabla e_\phi^{k-1}), P_\tau\overrightarrow{e}_u^k\rangle\right] \\
&\qquad + \lambda\left(\frac{\gamma_S}{\gamma_D}\right)^2\|\varepsilon_D^{k-1}\|_\Gamma^2 + \lambda\left[1-\left(\frac{\gamma_S}{\gamma_D}\right)^2\right]\|g e_\phi^{k-1}\|_\Gamma^2 \\
&\qquad - 2\lambda\gamma_S\left(1+\frac{\gamma_S}{\gamma_D}\right) g\, a_D(e_\phi^{k-1}, e_\phi^{k-1}) + \lambda(\gamma_D^2-\gamma_S^2)\|\overrightarrow{e}_u^k\cdot\overrightarrow{n}_S\|_\Gamma^2 \\
&= -2(\gamma_S+\gamma_D)\left[\lambda c_S(\overrightarrow{e}_u^k, \overrightarrow{u}_S, \overrightarrow{e}_u^k) + \lambda c_S(\overrightarrow{u}_S, \overrightarrow{e}_u^k, \overrightarrow{e}_u^k) + a_S(\overrightarrow{e}_u^k, \overrightarrow{e}_u^k)\right. \\
&\qquad \left. + \lambda g\, a_D(e_\phi^{k-1}, e_\phi^{k-1}) + \frac{\alpha\sqrt{\mathbf{d}}}{\sqrt{\operatorname{trace}(\prod)}}\langle P_\tau(\overrightarrow{e}_u^k + \mathbb{K}\nabla e_\phi^{k-1}), P_\tau\overrightarrow{e}_u^k\rangle\right] \\
&\qquad + \lambda\left(\frac{\gamma_S}{\gamma_D}\right)^2\|\varepsilon_D^{k-1}\|_\Gamma^2 + \lambda\left[1-\left(\frac{\gamma_S}{\gamma_D}\right)^2\right]\|g e_\phi^{k-1}\|_\Gamma^2 \\
&\qquad + 2\lambda(\gamma_S+\gamma_D)\left(1-\frac{\gamma_S}{\gamma_D}\right) g\, a_D(e_\phi^{k-1}, e_\phi^{k-1}) + \lambda(\gamma_D^2-\gamma_S^2)\|\overrightarrow{e}_u^k\cdot\overrightarrow{n}_S\|_\Gamma^2.
\end{aligned} \tag{6.28}$$

Plugging (6.15), (6.22), and (6.23) into (6.28), we obtain

$$\lambda\|\varepsilon_D^{k+1}\|_\Gamma^2 \le -2(\gamma_S+\gamma_D)C_1\left[a_S(\overrightarrow{e}_u^k, \overrightarrow{e}_u^k) + \lambda g a_D(e_\phi^{k-1}, e_\phi^{k-1})\right] + \lambda\left(\frac{\gamma_S}{\gamma_D}\right)^2\|\varepsilon_D^{k-1}\|_\Gamma^2$$

$$+\lambda\left[1-\left(\frac{\gamma_S}{\gamma_D}\right)^2\right]g^2\frac{C_4}{K}a_D(e_\phi^{k-1},e_\phi^{k-1})$$

$$+2\lambda(\gamma_S+\gamma_D)\left(1-\frac{\gamma_S}{\gamma_D}\right)ga_D(e_\phi^{k-1},e_\phi^{k-1})+\lambda(\gamma_D^2-\gamma_S^2)C_3a_S(\overrightarrow{e}_u^k,\overrightarrow{e}_u^k). \tag{6.29}$$

For a constant $s\in(0,2)$, we have

$$\begin{aligned}\lambda\|\varepsilon_D^{k+1}\|_\Gamma^2+(2-s)(\gamma_S+\gamma_D)C_1\left[a_S(\overrightarrow{e}_u^k,\overrightarrow{e}_u^k)+\lambda ga_D(e_\phi^{k-1},e_\phi^{k-1})\right]\\ \le\lambda\left(\frac{\gamma_S}{\gamma_D}\right)^2\|\varepsilon_D^{k-1}\|_\Gamma^2+\left[\lambda(\gamma_D^2-\gamma_S^2)C_3-s(\gamma_S+\gamma_D)C_1\right]a_S(\overrightarrow{e}_u^k,\overrightarrow{e}_u^k)\\ +\left\{\left[1-\left(\frac{\gamma_S}{\gamma_D}\right)^2\right]g\frac{C_4}{K}+2(\gamma_S+\gamma_D)\left(1-\frac{\gamma_S}{\gamma_D}\right)-s(\gamma_S+\gamma_D)C_1\right\}\\ \lambda ga_D(e_\phi^{k-1},e_\phi^{k-1}).\end{aligned} \tag{6.30}$$

Choose γ_S and γ_D such that

$$\lambda(\gamma_D^2-\gamma_S^2)C_3-s(\gamma_S+\gamma_D)C_1\le 0, \tag{6.31}$$

$$\left[1-\left(\frac{\gamma_S}{\gamma_D}\right)^2\right]g\frac{C_4}{K}+2(\gamma_S+\gamma_D)\left(1-\frac{\gamma_S}{\gamma_D}\right)-s(\gamma_S+\gamma_D)C_1\le 0. \tag{6.32}$$

Then we obtain

$$\begin{aligned}\lambda\|\varepsilon_D^{k+1}\|_\Gamma^2+(2-s)(\gamma_S+\gamma_D)C_1\left[a_S(\overrightarrow{e}_u^k,\overrightarrow{e}_u^k)+\lambda ga_D(e_\phi^{k-1},e_\phi^{k-1})\right]\\ \le\lambda\left(\frac{\gamma_S}{\gamma_D}\right)^2\|\varepsilon_D^{k-1}\|_\Gamma^2.\end{aligned} \tag{6.33}$$

This provides the geometric convergence rate $\sqrt{\frac{\gamma_S}{\gamma_D}}$. Here the requirements (6.31)–(6.32) are equivalent to

$$\gamma_D-\gamma_S\le\frac{sC_1}{\lambda C_3}, \tag{6.34}$$

$$\gamma_D-\gamma_S\le\frac{sC_1\gamma_D^2K}{gC_4+2\gamma_DK}. \tag{6.35}$$

Using (6.3), we can obtain the geometric convergence for e_p^k. ∎

7. Numerical examples. In this section, we will present three examples to illustrate the features of the proposed method. Newton iteration will be used to deal with the nonlinear systems. The Taylor–Hood element pair will be used for the Navier–Stokes equations, and the quadratic finite element will be used for the second order formulation of the Darcy equation.

Example 1. Consider the model problem (2.3)–(2.8) on $\Omega=[0,1]\times[0,1]$. Let Ω_S be the polygon $\overline{ABCDEFGHIJ}$, where $A=(0,1)$, $B=(0,3/4)$, $C=(1/2,1/4)$, $D=(1/2,0)$, $E=(3/4,0)$, $F=(3/4,1/4)$, $G=(1,1/4)$, $H=(1,1/2)$, $I=(3/4,1/2)$, and $J=(1/4,1)$. Let $\Omega_D=\Omega/\Omega_S$ and $\Gamma=\overline{\Omega}_D\cap\overline{\Omega}_S$.

Choose $\alpha\nu\sqrt{\mathbf{d}}/\sqrt{\mathrm{trace}(\prod)}=1$, $\nu=1$, $g=1$, $z=0$, and $\mathbb{K}=K\mathbb{I}$, where $\mathbb{I}$ is the identity matrix and $K=1$. Let $\overrightarrow{f}_S=0$ in Ω_S, $f_D=0$ in Ω_D, and $\phi_D=0$ on $\partial\Omega_D/\Gamma$. Let

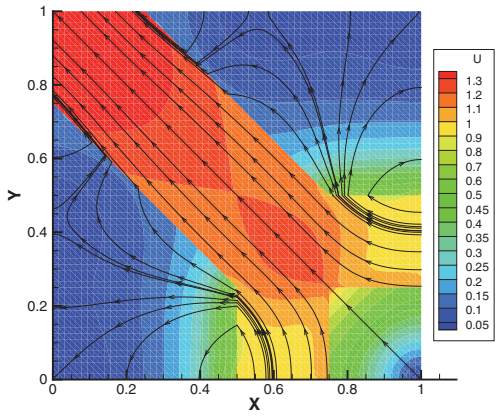

FIG. 2. *Example* 1: *Plot of the speed and the streamlines of the velocity for* $s_1 = 1$ *and* $s_2 = 1$.

$$\overrightarrow{u}_S = \begin{cases} (-s_1, 0)^T & \text{on } \overline{GH}, \\ (0, s_1)^T & \text{on } \overline{DE}, \\ (-s_2, s_2)^T & \text{on } \overline{AB} \text{ and } \overline{JA}, \end{cases}$$

where s_1 and s_2 are two constants. We divide Ω into rectangles of height and width $h = 1/N$, where N denotes a positive integer, and then subdivide each rectangle into two triangles by drawing a diagonal. N is chosen such that the boundary of Ω_S is aligned with the mesh. Clearly, faces of the grids in Ω_D and Ω_S align with and match at the interface $\Gamma = \Omega_D \bigcap \Omega_S$.

For the proposed DDM, we choose $\gamma_S = 0.3$, $\gamma_D = 1.2$, and $N = 64$. In the following, we will first discuss the effect of different boundary data in order to validate the proposed numerical method. First, Figure 2 shows the simulation results for $s_1 = 1$ and $s_2 = 1$, where the warmer color indicates higher speed of the flow, and the line with arrows is the streamline. In this case, the total inflow rate is equal to the total outflow rate. Second, we choose $s_1 = 1$ and $s_2 = 1/2$, which cause the total inflow rate to be larger than the total outflow rate. Then the simulation results in Figure 3 show that the flow becomes slower in the left-top quarter of the problem domain. By comparing the contours and the streamlines in Figure 3 with those in Figure 2, it is seen that more fluid flows out of the conduit to the porous media region. Indeed, none of the streamlines, which go from the conduit to the porous media, come back to the conduit. Third, we choose $s_1 = 1$ and $s_2 = 3/2$, which cause the total inflow rate to be larger than the total outflow rate in Figure 4. In the left-top quarter of the problem domain, the flow becomes faster. Compared with Figure 2, it can be seen that more fluid flows from a broader porous media area into the free flow region.

Furthermore, we change K to be 10^{-2}, 10^{-4}, 10^{-6} in this example to test the effect of smaller K on the solution. Figures 5, 6, and 7 show that the domain decomposition solutions are convergent for these smaller values of K, and the flow speed in porous media is significantly reduced when K becomes smaller. Comparing with Figure 2, the slower flow in porous media also causes a smaller effect of the porous media flow on the fluid flow in the region around the interface. In order to illustrate more details for the porous media flow, smaller scales are used for smaller K in Figures 6 and 7.

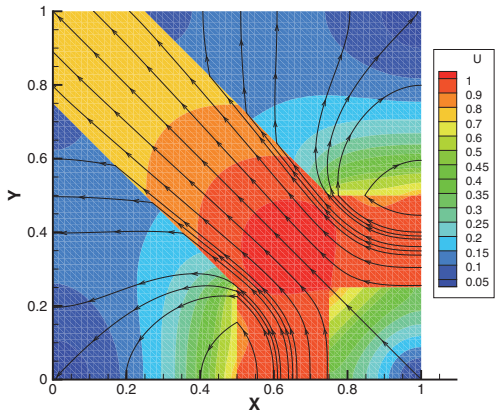

FIG. 3. *Example* 1: *Plot of the speed and the streamlines of the velocity for* $s_1 = 1$ *and* $s_2 = 1/2$.

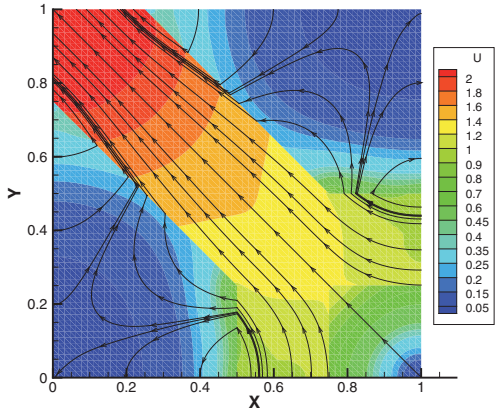

FIG. 4. *Example* 1: *Plot of the speed and the streamlines of the velocity for* $s_1 = 1$, $s_2 = 3/2$, *and* $K = 1$.

Example 2. Consider the model problem (2.3)–(2.8) without the inertial force $\frac{1}{2}\overrightarrow{u}_S \cdot \overrightarrow{u}_S$ on the interface. The source terms and boundary conditions are chosen such that the exact solution is given by

$$\begin{cases} \phi_D = [2 - \pi \sin(\pi x)][-y + \cos(\pi(1-y))], \\ \overrightarrow{u}_S = [x^2y^2 + e^{-y}, \ -\frac{2}{3}xy^3 + 2 - \pi \sin(\pi x)]^T, \\ p_S = -[2 - \pi \sin(\pi x)] \cos(2\pi y). \end{cases}$$

The problem domain is $\Omega = [0,1] \times [-0.25, 0.75]$, where $\Omega_D = [0,1] \times [0, 0.75]$ and $\Omega_S = [0,1] \times [-0.25, 0]$. Choose $\alpha\nu\sqrt{\mathbf{d}}/\sqrt{\text{trace}(\prod)} = 1$, $\nu = 1$, $g = 1$, and $\mathbb{K} = K\mathbb{I}$, where $\mathbb{I}$ is the identity matrix and $K = 1$. We divide Ω_D and Ω_S into rectangles of height and width $h = 1/N$, where N denotes a positive integer, and then subdivide each rectangle into two triangles by drawing a diagonal. In this example, we will illustrate the accuracy order and convergence of the proposed method.

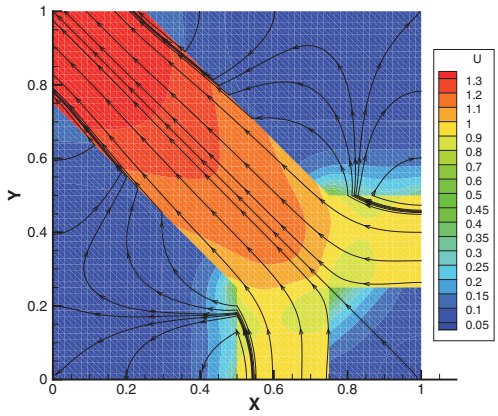

FIG. 5. *Example* 1: *Plot of the speed and the streamlines of the velocity for* $s_1 = 1$, $s_2 = 1$, *and* $K = 10^{-2}$.

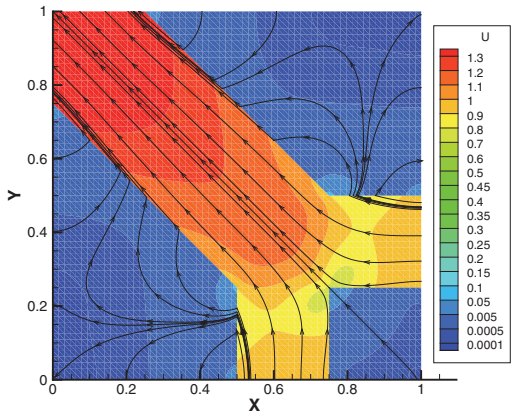

FIG. 6. *Example* 1: *Plot of the speed and the streamlines of the velocity for* $s_1 = 1$, $s_2 = 1$, *and* $K = 10^{-4}$.

For the coupled finite element method corresponding to the coupled weak formulation (3.1), Table 1 provides errors for different choices of h. Using linear regression, the errors in Table 1 satisfy

$$\|\overrightarrow{u}_{S,h} - \overrightarrow{u}_S\|_0 \approx 0.177\ h^{2.998}, \qquad |\overrightarrow{u}_{S,h} - \overrightarrow{u}_S|_1 \approx 1.281\ h^{1.999},$$
$$\|p_{S,h} - p_S\|_0 \approx 1.264\ h^{2.018},$$
$$\|\phi_{D,h} - \phi_D\|_0 \approx 0.545\ h^{3.002}, \qquad |\phi_{D,h} - \phi_D|_1 \approx 4.515\ h^{1.995}.$$

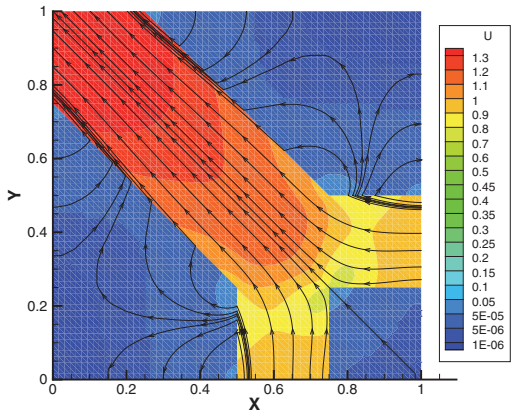

FIG. 7. *Example* 1: *Plot of the speed and the streamlines of the velocity for* $s_1 = 1$, $s_2 = 1$, *and* $K = 10^{-6}$.

TABLE 1
Example 2: *Errors of the finite element method.*

h	$\|\overrightarrow{u}_{S,h} - \overrightarrow{u}_S\|_0$	$\|\overrightarrow{u}_{S,h} - \overrightarrow{u}_S\|_1$	$\|p_{S,h} - p_S\|_0$	$\|\phi_{D,h} - \phi_D\|_0$	$\|\phi_{D,h} - \phi_D\|_1$
1/8	3.488×10^{-4}	2.009×10^{-2}	1.941×10^{-2}	1.063×10^{-3}	7.088×10^{-2}
1/16	4.325×10^{-5}	5.012×10^{-3}	4.648×10^{-3}	1.319×10^{-4}	1.796×10^{-2}
1/32	5.424×10^{-6}	1.255×10^{-3}	1.139×10^{-3}	1.645×10^{-5}	4.511×10^{-3}
1/64	6.804×10^{-7}	3.143×10^{-4}	2.831×10^{-4}	2.056×10^{-6}	1.130×10^{-3}
1/128	8.525×10^{-8}	7.866×10^{-5}	7.065×10^{-5}	2.571×10^{-7}	2.827×10^{-4}
1/256	1.067×10^{-8}	1.968×10^{-5}	1.765×10^{-5}	3.214×10^{-8}	7.069×10^{-5}

These rates of convergence are consistent with the approximation capability of the Taylor–Hood element and quadratic element. In particular, we see the third order convergence rate with respect to the L^2 norm of $\overrightarrow{u}_S$ and ϕ_D, the second order convergence rates with respect to the H^1 norm of $\overrightarrow{u}_S$ and ϕ_D, and the second order convergence rate with respect to L^2 norms of p_S.

For the DDM with $\gamma_S = 0.3$ and $h = 1/32$, Figures 8 and 9 show the L^2 errors of hydraulic head, velocity, pressure, and η_S. In order to obtain the convergence of the DDM, the requirements in Theorem 6.4 need to be satisfied. We can see that for this example the proposed DDM is convergent for $\gamma_D = \gamma_S$ and $\gamma_D = 4\gamma_S$ but not $\gamma_D = \frac{1}{4}\gamma_S$.

Remark 7.1. In this section, we remove the error from the initial guess of the DDM iteration and start from the error of the first DDM iteration step as the "step 0" in the plots.

In addition to the above observation about the convergence, we also observe a geometric convergence rate $\sqrt{\frac{\gamma_S}{\gamma_D}}$ for the case of $\gamma_S < \gamma_D$. First, it is observed that smaller $\frac{\gamma_S}{\gamma_D}$ provides faster convergence in Figures 10 and 11 when the requirements of Theorem 6.4 are satisfied. Then Tables 2 and 3 list some L^2 errors in velocity, hydraulic head, pressure, and η_S for the proposed DDM with $\gamma_S = 0.3$ and $\gamma_D = 1.2$. Let $e(i)$ denote the error at the ith iteration step. We can see that all the error ratios are less than $\left(\sqrt{\frac{\gamma_S}{\gamma_D}}\right)^4 = \left(\sqrt{\frac{1}{4}}\right)^4 = 0.0625$, which numerically confirms the geometric

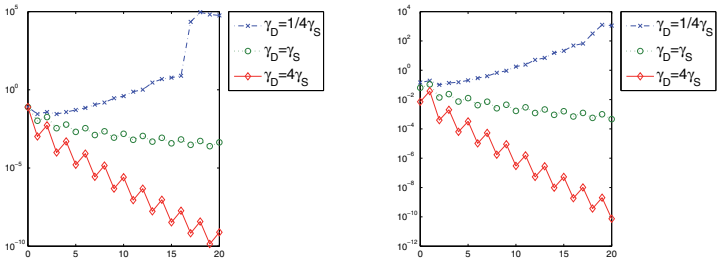

FIG. 8. *Example* 2: *Convergence for the velocity of the free flow (left) and the hydraulic head of the porous medium flow (right) versus the iteration counter* m *for the DDM.*

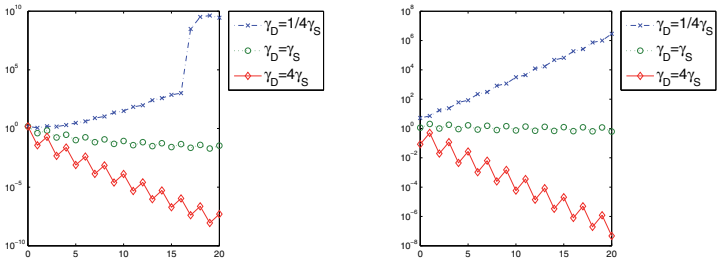

FIG. 9. *Example* 2: *Convergence for the pressure of the free flow (left) and* η_S *(right) versus the iteration counter* m *for the DDM.*

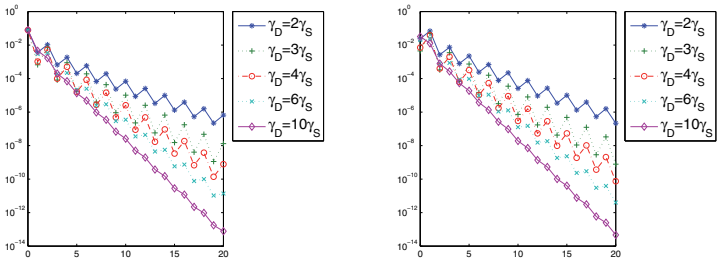

FIG. 10. *Example* 2: *Geometric convergence rate of the velocity of the free flow (left) and the hydraulic head of the porous medium flow (right) for the DDM.*

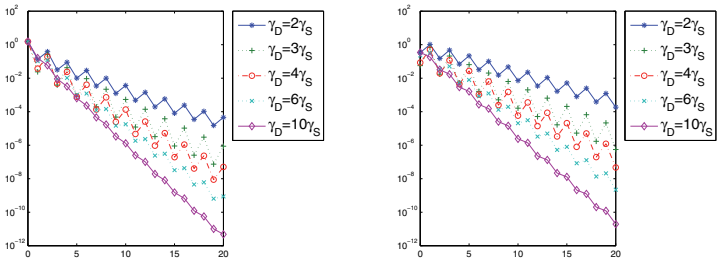

FIG. 11. *Example* 2: *Geometric convergence rate of the pressure of the free flow (left) and* η_S *(right) versus the iteration counter* m *for the DDM.*

TABLE 2
Example 2: L^2 *errors in velocity and hydraulic head for the DDM.*

	L^2 velocity errors	$\frac{e(i)}{e(i-4)}$	L^2 hydraulic head errors	$\frac{e(i)}{e(i-4)}$
$e(0)$	7.873×10^{-2}		7.104×10^{-3}	
$e(4)$ $(i = 4)$	5.023×10^{-4}	0.00638	6.318×10^{-5}	0.00889
$e(8)$ $(i = 8)$	1.437×10^{-5}	0.0286	1.727×10^{-6}	0.0273
$e(12)$ $(i = 12)$	4.801×10^{-7}	0.0334	5.298×10^{-8}	0.0307
$e(16)$ $(i = 16)$	1.846×10^{-8}	0.0384	1.864×10^{-9}	0.0352
$e(20)$ $(i = 20)$	7.791×10^{-10}	0.0422	7.399×10^{-11}	0.0397

TABLE 3
Example 2: L^2 *errors in pressure and* η_S *for the DDM.*

	L^2 velocity errors	$\frac{e(i)}{e(i-4)}$	L^2 hydraulic head errors	$\frac{e(i)}{e(i-4)}$
$e(0)$	1.534×10^{0}		8.468×10^{-2}	
$e(4)$ $(i = 4)$	2.394×10^{-2}	0.0156	4.486×10^{-3}	0.0530
$e(8)$ $(i = 8)$	7.204×10^{-4}	0.0301	2.454×10^{-4}	0.0547
$e(12)$ $(i = 12)$	2.586×10^{-5}	0.0359	1.386×10^{-5}	0.0558
$e(16)$ $(i = 16)$	1.087×10^{-6}	0.0420	8.005×10^{-7}	0.0585
$e(20)$ $(i = 20)$	5.054×10^{-8}	0.0465	4.699×10^{-8}	0.0587

convergence rate $\sqrt{\frac{\gamma_S}{\gamma_D}}$.

Additionally, we have similar observations for the errors in other norms, including the errors of hydraulic head and velocity in the H^1 norm and discrete maximum norm and the errors of pressure and η_S in the discrete maximum norm. Hence, we omit the related data here in order to simplify the presentation.

Example 3. Consider the model problem (2.3)–(2.8). The source terms and boundary conditions are chosen such that the exact solution is given by

$$\begin{cases} \phi_D = (e^y + e^{-y} - 2)\sin(x), \\ \overrightarrow{u}_S = \left[K\left(\frac{1}{\pi}\sin(2\pi y) - 2y\right)\cos(x),\ K\left(\frac{1}{\pi^2}\sin^2(\pi y) - y^2\right)\sin(x)\right]^T, \\ p_S = 0. \end{cases}$$

The problem domain is $\Omega = [0, \pi] \times [-1, 1]$, where $\Omega_D = [0, \pi] \times [-1, 0]$ and $\Omega_S = [0, \pi] \times [0, 1]$. Choose $\alpha\nu\sqrt{\mathbf{d}}/\sqrt{\text{trace}(\prod)} = 1$, $\nu = 1$, $g = 1$, and $\mathbb{K} = K\mathbb{I}$, where $\mathbb{I}$ is the identity matrix. We divide Ω_D and Ω_S into rectangles of height and width $h = (\pi/N, 1/N)$, where N denotes a positive integer, and then subdivide each rectangle into two triangles by drawing a diagonal. In this example, we will illustrate the influence of the parameter K on the convergence and convergence rate since the given analytic solutions satisfy the interface conditions (2.6)–(2.8) for arbitrary K. Again, in the figures we remove the error from the initial guess of the DDM iteration and start from the error of the first DDM iteration step as "step 0."

Figures 12–15 show the convergence and convergence rate of the hydraulic head for different choices on K, γ_D, and γ_S. The figures for the velocity of the free flow are similar; hence they are omitted here to shorten the presentation. As indicated in (6.35), we can see that the parameter K does have a significant influence on the choice of the parameters γ_D and γ_S for the convergence and convergence rate. Smaller K requires larger γ_D and γ_S for a better performance in convergence and convergence rate, which is consistent with the nonlinear requirement in (6.35). The errors in Figures 12–15 quickly decrease for $K = 1,\ 10^{-2},\ 10^{-4},\ 10^{-6}$. Therefore the convergence rate is good for smaller K even though it is not as good as the case of $K = 1$ due to some nonlinear effect of the smaller K on the convergence and convergence rate,

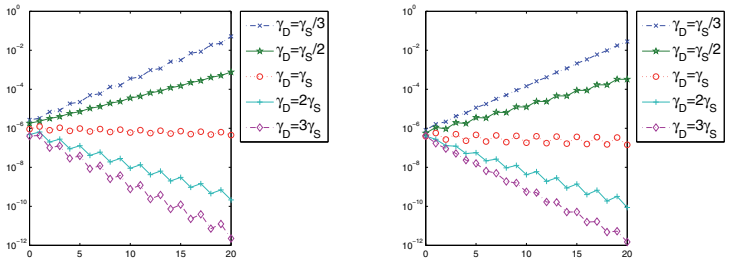

FIG. 12. *Example* 3: *Convergence and convergence rate of the hydraulic head for* $K = 1$ *with* $\gamma_S = 0.3$ *(left) and* $\gamma_S = 1$ *(right).*

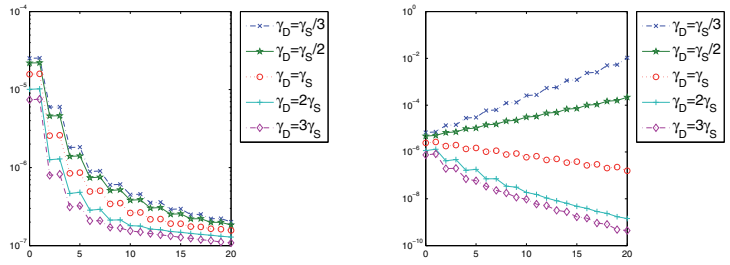

FIG. 13. *Example* 3: *Convergence and convergence rate of the hydraulic head for* $K = 10^{-2}$ *with* $\gamma_S = 1$ *(left) and* $\gamma_S = 10$ *(right).*

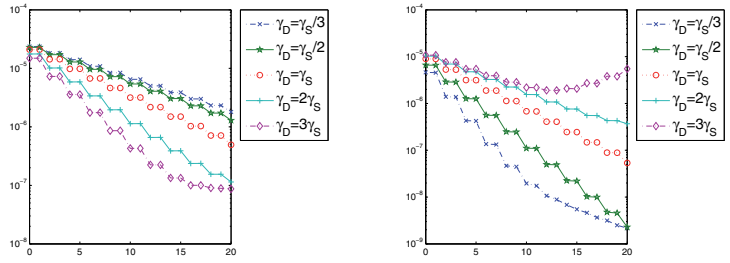

FIG. 14. *Example* 3: *Convergence and convergence rate of the hydraulic head for* $K = 10^{-4}$ *with* $\gamma_S = 10$ *(left) and* $\gamma_S = 1000$ *(right).*

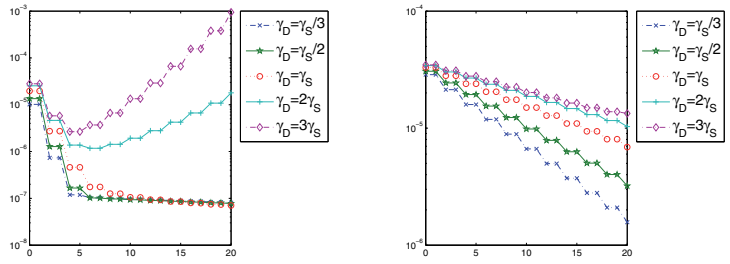

FIG. 15. *Example* 3: *Convergence and convergence rate of the hydraulic head for* $K = 10^{-6}$ *with* $\gamma_S = 10000$ *(left) and* $\gamma_S = 100000$ *(right).*

which will lead to some interesting future work.

8. Conclusions. In this paper, the well-posedness of the coupled weak formulation for the stationary Naiver–Stokes–Darcy model with Beavers–Joseph interface condition is illustrated by using a branch of nonsingular solutions. Then a multiphysics domain decomposition method is proposed and analyzed for this model based on the Robin boundary conditions constructed from the three physical interface conditions. The numerical experiments validate the proposed method and verify the theoretical conclusions.

REFERENCES

[1] P. J. Alvarez and W. A. Illman, *Bioremediation and Natural Attenuation: Process Fundamentals and Mathematical Models*, Wiley Interscience, New York, 2006.

[2] T. Arbogast and D. S. Brunson, *A computational method for approximating a Darcy-Stokes system governing a vuggy porous medium*, Comput. Geosci., 11 (2007), pp. 207–218.

[3] T. Arbogast and M. Gomez, *A discretization and multigrid solver for a Darcy-Stokes system of three dimensional vuggy porous media*, Comput. Geosci., 13 (2009), pp. 331–348.

[4] T. Arbogast and H. L. Lehr, *Homogenization of a Darcy-Stokes system modeling vuggy porous media*, Comput. Geosci., 10 (2006), pp. 291–302.

[5] I. Babuška and G. N. Gatica, *A residual-based a posteriori error estimator for the Stokes–Darcy coupled problem*, SIAM J. Numer. Anal., 48 (2010), pp. 498–523.

[6] L. Badea, M. Discacciati, and A. Quarteroni, *Numerical analysis of the Navier-Stokes/Darcy coupling*, Numer. Math., 115 (2010), pp. 195–227.

[7] G. E. Barenblatt, I. P. Zheltov, and I. N. Kochina, *Basic concepts in the theory of homogeneous liquids in fissured rocks*, J. Appl. Math. Mech., 24 (1960), pp. 1286–1303.

[8] G. Beavers and D. Joseph, *Boundary conditions at a naturally permeable wall*, J. Fluid Mech., 30 (1967), pp. 197–207.

[9] Y. Boubendir and S. Tlupova, *Stokes-Darcy boundary integral solutions using preconditioners*, J. Comput. Phys., 228 (2009), pp. 8627–8641.

[10] Y. Boubendir and S. Tlupova, *Domain decomposition methods for solving Stokes–Darcy problems with boundary integrals*, SIAM J. Sci. Comput., 35 (2013), pp. B82–B106.

[11] M. Cai and M. Mu, *A multilevel decoupled method for a mixed Stokes/Darcy model*, J. Comput. Appl. Math., 236 (2012), pp. 2452–2465.

[12] M. Cai, M. Mu, and J. Xu, *Numerical solution to a mixed Navier–Stokes/Darcy model by the two-grid approach*, SIAM J. Numer. Anal., 47 (2009), pp. 3325–3338.

[13] A. Caiazzo, V. John, and U. Wilbrandt, *On classical iterative subdomain methods for the Stokes-Darcy problem*, Comput. Geosci., 18 (2014), pp. 711–728.

[14] S. Cao, J. Pollastrini, and Y. Jiang, *Separation and characterization of protein aggregates and particles by field flow fractionation*, Curr. Pharm. Biotechnol., 10 (2009), pp. 382–390.

[15] Y. Cao, Y. Chu, X. He, and M. Wei, *Decoupling the stationary Navier-Stokes-Darcy system with the Beavers-Joseph-Saffman interface condition*, Abstr. Appl. Anal., 2013, 136483.

[16] Y. Cao, M. Gunzburger, X.-M. He, and X. Wang, *Robin-Robin domain decomposition methods for the steady Stokes-Darcy model with Beaver-Joseph interface condition*, Numer. Math., 117 (2011), pp. 601–629.

[17] Y. Cao, M. Gunzburger, X.-M. He, and X. Wang, *Parallel, non-iterative, multi-physics domain decomposition methods for time-dependent Stokes-Darcy systems*, Math. Comp., 83 (2014), pp. 1617–1644.

[18] Y. Cao, M. Gunzburger, X. Hu, F. Hua, X. Wang, and W. Zhao, *Finite element approximations for Stokes–Darcy flow with Beavers–Joseph interface conditions*, SIAM. J. Numer. Anal., 47 (2010), pp. 4239–4256.

[19] Y. Cao, M. Gunzburger, F. Hua, and X. Wang, *Coupled Stokes-Darcy model with Beavers-Joseph interface boundary condition*, Comm. Math. Sci., 8 (2010), pp. 1–25.

[20] A. Çeşmelioğlu, V. Girault, and B. Rivière, *Time-dependent coupling of Navier-Stokes and Darcy flows*, ESAIM Math. Model. Numer. Anal., 47 (2013), pp. 539–554.

[21] A. Çeşmelioğlu and B. Rivière, *Analysis of time-dependent Navier-Stokes flow coupled with Darcy flow*, J. Numer. Math., 16 (2008), pp. 249–280.

[22] A. Çeşmelioğlu and B. Rivière, *Primal discontinuous Galerkin methods for time-dependent coupled surface and subsurface flow*, J. Sci. Comput., 40 (2009), pp. 115–140.

[23] J. Chen, S. Sun, and X. Wang, *A numerical method for a model of two-phase flow in a coupled free flow and porous media system*, J. Comput. Phys., 268 (2014), pp. 1–16.
[24] N. Chen, M. Gunzburger, and X. Wang, *Asymptotic analysis of the differences between the Stokes-Darcy system with different interface conditions and the Stokes-Brinkman system*, J. Math. Anal. Appl., 368 (2010), pp. 658–676.
[25] W. Chen, P. Chen, M. Gunzburger, and N. Yan, *Superconvergence analysis of FEMs for the Stokes-Darcy system*, Math. Methods Appl. Sci., 33 (2010), pp. 1605–1617.
[26] W. Chen, M. Gunzburger, F. Hua, and X. Wang, *A parallel Robin–Robin domain decomposition method for the Stokes–Darcy system*, SIAM. J. Numer. Anal., 49 (2011), pp. 1064–1084.
[27] W. Chen, M. Gunzburger, D. Sun, and X. Wang, *Efficient and long-time accurate second-order methods for the Stokes–Darcy system*, SIAM J. Numer. Anal., 51 (2013), pp. 2563–2584.
[28] W. Chen and Y. Wang, *A posteriori error estimate for the H(div) conforming mixed finite element for the coupled Darcy–Stokes system*, J. Comput. Appl. Math., 255 (2014), pp. 502–516.
[29] Z. Chen, Z. Wang, L. Zhu, and J. Li, *Analysis of the pressure projection stabilization method for the Darcy and coupled Darcy–Stokes flows*, Comput. Geosci., 17 (2013), pp. 1079–1091.
[30] P. Chidyagwai and R. B. Rivière, *On the solution of the coupled Navier-Stokes and Darcy equations*, Comput. Methods Appl. Mech. Engrg., 198 (2009), pp. 3806–3820.
[31] M. Cui and N. Yan, *A posteriori error estimate for the Stokes-Darcy system*, Math. Methods Appl. Sci., 34 (2011), pp. 1050–1064.
[32] C. D'Angelo and P. Zunino, *Numerical approximation with Nitsche's coupling of transient Stokes'/Darcy's flow problems applied to hemodynamics*, Appl. Numer. Math., 62 (2012), pp. 378–395.
[33] M. Discacciati, *Domain Decomposition Methods for the Coupling of Surface and Groundwater Flows*, Ph.D. thesis, Ecole Polytechnique Fédérale de Lausanne, Lausanne, Switzerland, 2004.
[34] M. Discacciati, *Iterative methods for Stokes/Darcy coupling*, in Domain Decomposition Methods in Science and Engineering, Lect. Notes Comput. Sci. Eng. 40, Springer, Berlin, 2005, pp. 563–570.
[35] M. Discacciati, E. Miglio, and A. Quarteroni, *Mathematical and numerical models for coupling surface and groundwater flows*, Appl. Numer. Math., 43 (2002), pp. 57–74.
[36] M. Discacciati and A. Quarteroni, *Analysis of a domain decomposition method for the coupling of Stokes and Darcy equations*, in Numerical Mathematics and Advanced Applications, Springer Italia, Milan, 2003, pp. 3–20.
[37] M. Discacciati and A. Quarteroni, *Convergence analysis of a subdomain iterative method for the finite element approximation of the coupling of Stokes and Darcy equations*, Comput. Vis. Sci., 6 (2004), pp. 93–103.
[38] M. Discacciati and A. Quarteroni, *Navier-Stokes/Darcy coupling: Modeling, analysis, and numerical approximation*, Rev. Mat. Complut., 22 (2009), pp. 315–426.
[39] M. Discacciati, A. Quarteroni, and A. Valli, *Robin–Robin domain decomposition methods for the Stokes–Darcy coupling*, SIAM J. Numer. Anal., 45 (2007), pp. 1246–1268.
[40] V. J. Ervin, *Approximation of coupled Stokes–Darcy flow in an axisymmetric domain*, Comput. Methods Appl. Mech. Engrg., 258 (2013), pp. 96–108.
[41] V. J. Ervin, E. W. Jenkins, and H. Lee, *Approximation of the Stokes-Darcy system by optimization*, J. Sci. Comput., 59 (2014), pp. 775–794.
[42] V. J. Ervin, E. W. Jenkins, and S. Sun, *Coupled generalized nonlinear Stokes flow with flow through a porous medium*, SIAM J. Numer. Anal., 47 (2009), pp. 929–952.
[43] V. J. Ervin, E. W. Jenkins, and S. Sun, *Coupling nonlinear Stokes and Darcy flow using mortar finite elements*, Appl. Numer. Math., 61 (2011), pp. 1198–1222.
[44] M.-F. Feng, R.-S. Qi, R. Zhu, and B.-T. Ju, *Stabilized Crouzeix-Raviart element for the coupled Stokes and Darcy problem*, Appl. Math. Mech. (English Ed.), 31 (2010), pp. 393–404.
[45] W. Feng, X.-M. He, Z. Wang, and X. Zhang, *Non-iterative domain decomposition methods for a non-stationary Stokes-Darcy model with Beavers-Joseph interface condition*, Appl. Math. Comput., 219 (2012), pp. 453–463.
[46] K. M. Fisher, *The effects of fluid flow on solidification of industrial castings and ingots*, Phys. Chem. Hydrodyn., 2 (1981), pp. 311–326.
[47] W. Fraunhofer and G. Winter, *The use of asymmetrical flow field-flow fractionation in pharmaceutics and biopharmaceutics*, Eur. J. Pharm. Biopharm., 58 (2004), pp. 369–383.
[48] J. Galvis and M. Sarkis, *Balancing domain decomposition methods for mortar coupling Stokes-Darcy systems*, in Domain Decomposition Methods in Science and Engineering

XVI, Lect. Notes in Comput. Sci. Eng. 55, Springer, Berlin, 2007, pp. 373–380.
[49] J. Galvis and M. Sarkis, *Non-matching mortar discretization analysis for the coupling Stokes-Darcy equations*, Electron. Trans. Numer. Anal., 26 (2007), pp. 350–384.
[50] J. Galvis and M. Sarkis, *FETI and BDD preconditioners for Stokes-Mortar-Darcy systems*, Commun. Appl. Math. Comput. Sci., 5 (2010), pp. 1–30.
[51] G. N. Gatica, S. Meddahi, and R. Oyarzúa, *A conforming mixed finite-element method for the coupling of fluid flow with porous media flow*, IMA J. Numer. Anal., 29 (2009), pp. 86–108.
[52] G. N. Gatica, R. Oyarzúa, and F. J. Sayas, *A residual-based a posteriori error estimator for a fully-mixed formulation of the Stokes-Darcy coupled problem*, Comput. Methods Appl. Mech. Engrg., 200 (2011), pp. 1877–1891.
[53] G. N. Gatica, R. Oyarzúa, and F. J. Sayas, *Convergence of a family of Galerkin discretizations for the Stokes-Darcy coupled problem*, Numer. Methods Partial Differential Equations, 27 (2011), pp. 721–748.
[54] V. Girault, G. Kanschat, and B. Rivière, *Error analysis for a monolithic discretization of coupled Darcy and Stokes problems*, J. Numer. Math., 22 (2014), pp. 109–142.
[55] V. Girault and P. A. Raviart, *Finite Element Methods for Navier-Stokes Equations. Theory and Algorithms*, Springer Ser. Comput. Math. 5, Springer-Verlag, Berlin, 1986.
[56] V. Girault and B. Rivière, *DG approximation of coupled Navier–Stokes and Darcy equations by Beaver–Joseph–Saffman interface condition*, SIAM J. Numer. Anal, 47 (2009), pp. 2052–2089.
[57] V. Girault, D. Vassilev, and I. Yotov, *Mortar multiscale finite element methods for Stokes–Darcy flows*, Numer. Math., 127 (2014), pp. 93–165.
[58] J. K. Guest and J. H. Prévost, *Topology optimization of creeping fluid flows using a Darcy-Stokes finite element*, Int. J. Numer. Methods Eng., 66 (2006), pp. 461–484.
[59] P. Gui, J. C. Cunha, and L. B. Cunha, *A coupled model to simulate the fluid flow in the reservoir and horizontal wellbore*, in Proceedings of the Canadian International Petroleum Conference, Calgary, Alberta, Society of Petroleum Engineers, 2006, Document ID 2006-124.
[60] D. Han, D. Sun, and X. Wang, *Two-phase flows in karstic geometry*, Math. Methods Appl. Sci., 37 (2014), pp. 3048–3063.
[61] D. Han, X. Wang, and H. Wu, *Existence and uniqueness of global weak solutions to a Cahn-Hilliard-Stokes-Darcy system for two phase incompressible flows in karstic geometry*, J. Differential Equations, 257 (2014), pp. 3887–3933.
[62] N. Hanspal, A. Waghode, V. Nassehi, and R. Wakeman, *Numerical analysis of coupled Stokes/Darcy flow in industrial filtrations*, Transp. Porous Media, 64 (2006), pp. 73–101.
[63] A. R. Hasan and C. S. Kabir, *Fluid Flow and Heat Transfer in Wellbores*, Society of Petroleum Engineers, Richardson, TX, 2002.
[64] Y. He and J. Li, *A stabilized finite element method based on local polynomial pressure projection for the stationary Navier-Stokes equation*, Appl. Numer. Math., 58 (2008), pp. 1503–1514.
[65] R. Hoppe, P. Porta, and Y. Vassilevski, *Computational issues related to iterative coupling of subsurface and channel flows*, CALCOLO, 44 (2007), pp. 1–20.
[66] P. Huang and J. Chen, *Some low order nonconforming mixed finite elements combined with Raviart-Thomas elements for a coupled Stokes-Darcy model*, Jpn. J. Ind. Appl. Math., 30 (2013), pp. 565–584.
[67] P. Huang, J. Chen, and M. Cai, *A mixed and nonconforming FEM with nonmatching meshes for a coupled Stokes-Darcy model*, J. Sci. Comput., 53 (2012), pp. 377–394.
[68] B. Jiang, *A parallel domain decomposition method for coupling of surface and groundwater flows*, Comput. Methods Appl. Mech. Engrg., 198 (2009), pp. 947–957.
[69] Z. Kang, Y. Wu, J. Li, Y. Wu, J. Zhang, and G. Wang, *Modeling multiphase flow in naturally fractured vuggy petroleum reservoirs*, in Proceedings of the SPE Annual Technical Conference and Exhibition, San Antonio, TX, Society of Petroleum Engineers, 2006, Document ID 102356-MS.
[70] G. Kanschat and B. Riviére, *A strongly conservative finite element method for the coupling of Stokes and Darcy flow*, J. Comput. Phys., 229 (2010), pp. 5933–5943.
[71] T. Karper, K. A. Mardal, and R. Winther, *Unified finite element discretizations of coupled Darcy-Stokes flow*, Numer. Methods Partial Differential Equations, 25 (2009), pp. 311–326.
[72] S. Khabthani, L. Elasmi, and F. Feuillebois, *Perturbation solution of the coupled Stokes-Darcy problem*, Discrete Contin. Dyn. Syst. Ser. B, 15 (2011), pp. 971–990.
[73] C. A. Kossack and O. Gurpinar, *A methodology for simulation of vuggy and fractured reservoirs*, in Proceedings of the SPE Reservoir Simulation Symposium, Houston, TX,

Society of Petroleum Engineers, 2006, Document ID 66366-MS.
[74] W. J. Layton, F. Schieweck, and I. Yotov, *Coupling fluid flow with porous media flow*, SIAM J. Numer. Anal., 40 (2003), pp. 2195–2218.
[75] H. Lee and K. Rife, *Least squares approach for the time-dependent nonlinear Stokes-Darcy flow*, Comput. Math. Appl., 67 (2014), pp. 1806–1815.
[76] J. Li and Z. Chen, *Optimal L^2, H^1 and L^∞ analysis of finite volume methods for the stationary Navier-Stokes equations with large data*, Numer. Math., 126 (2014), pp. 75–101.
[77] J. Li, Z. Chen, and Y. He, *A stabilized multi-level method for non-singular finite volume solutions of the stationary 3D Navier-Stokes equations*, Numer. Math., 122 (2012), pp. 279–304.
[78] X. Li and H. Rui, *A rectangular mixed element method with continuous flux approximation for coupling Stokes and Darcy flows*, Appl. Math. Comput., 246 (2014), pp. 39–53.
[79] P.-L. Lions, *On the Schwarz alternating method.* III. *A variant for nonoverlapping subdomains*, in Proceedings of the Third International Symposium on Domain Decomposition Methods for Partial Differential Equations (Houston, TX, 1989), SIAM, Philadelphia, 1990, pp. 202–223.
[80] K. Lipnikov, D. Vassilev, and I. Yotov, *Discontinuous Galerkin and mimetic finite difference methods for coupled Stokes-Darcy flows on polygonal and polyhedral grids*, Numer. Math., 126 (2014), pp. 321–360.
[81] A. Márquez, S. Meddahi, and F. J. Sayas, *A decoupled preconditioning technique for a mixed Stokes-Darcy model*, J. Sci. Comput., 57 (2013), pp. 174–192.
[82] T. Masuoka, *Convective current in a horizontal layer divided by a permeable wall*, Bull. JSME, 17 (1974), pp. 225–237.
[83] M. Mu and J. Xu, *A two-grid method of a mixed Stokes–Darcy model for coupling fluid flow with porous media flow*, SIAM J. Numer. Anal., 45 (2007), pp. 1801–1813.
[84] M. Mu and X. Zhu, *Decoupled schemes for a non-stationary mixed Stokes-Darcy model*, Math. Comp., 79 (2010), pp. 707–731.
[85] S. Münzenmaier and G. Starke, *First-order system least squares for coupled Stokes–Darcy flow*, SIAM J. Numer. Anal., 49 (2011), pp. 387–404.
[86] K. Nafa, *Equal order approximations enriched with bubbles for coupled Stokes-Darcy problem*, J. Comput. Appl. Math., 270 (2014), pp. 275–282.
[87] V. Nassehi, *Modelling of combined Navier-Stokes and Darcy flows in crossflow membrane filtration*, Chem. Eng. Sci., 53 (1998), pp. 1253–1265.
[88] S. O. Norris and L. D. Piper, *Modeling fluid flow around horizontal wellbores*, in Proceedings of the SPE Annual Technical Conference and Exhibition, New Orleans, LA, Society of Petroleum Engineers, 1990, Document ID 20719-MS.
[89] G. Pacquaut, J. Bruchon, N. Moulin, and S. Drapier, *Combining a level-set method and a mixed stabilized $P1/P1$ formulation for coupling Stokes–Darcy flows*, Internat. J. Numer. Methods Fluids, 69 (2012), pp. 459–480.
[90] W. Peng, G. Cao, Z. Dong, and S. Li, *Darcy-Stokes equations with finite difference and natural boundary element coupling method*, CMES Comput. Model. Eng. Sci., 75 (2011), pp. 173–188.
[91] D. Poulikakos and M. Kazmierczak, *Forced convection in a duct partially filled with a porous material*, J. Heat Transfer, 109 (1987), pp. 653–662.
[92] C. Pozrikidis and D. A. Farrow, *A model of fluid flow in solid tumors*, Ann. Biomed. Eng., 31 (2003), pp. 181–194.
[93] P. Reschiglian and M. H. Moon, *Flow field-flow fractionation: A pre-analytical method for proteomics*, J. Proteomics, 71 (2008), pp. 265–276.
[94] B. Rivière, *Analysis of a discontinuous finite element method for the coupled Stokes and Darcy problems*, J. Sci. Comput., 22/23 (2005), pp. 479–500.
[95] B. Rivière and I. Yotov, *Locally conservative coupling of Stokes and Darcy flows*, SIAM J. Numer. Anal., 42 (2005), pp. 1959–1977.
[96] H. Rui and R. Zhang, *A unified stabilized mixed finite element method for coupling Stokes and Darcy flows*, Comput. Methods Appl. Mech. Engrg., 198 (2009), pp. 2692–2699.
[97] I. Rybak and J. Magiera, *A multiple-time-step technique for coupled free flow and porous medium systems*, J. Comput. Phys., 272 (2014), pp. 327–342.

[98] A. G. Salinger, R. Aris, and J. J. Derby, *Finite element formulations for large-scale, coupled flows in adjacent porous and open fluid domains*, Int. J. Numer. Methods Fluids, 18 (1994), pp. 1185–1209.

[99] L. Shan and H. Zheng, *Partitioned time stepping method for fully evolutionary Stokes–Darcy flow with Beavers–Joseph interface conditions*, SIAM J. Numer. Anal., 51 (2013), pp. 813–839.

[100] L. Shan, H. Zheng, and W. Layton, *A decoupling method with different sub-domain time steps for the nonstationary Stokes-Darcy model*, Numer. Methods Partial Differential Equations, 29 (2013), pp. 549–583.

[101] Z. Si, Y. Wang, and S. Li, *Decoupled modified characteristics finite element method for the time dependent Navier-Stokes/Darcy problem*, Math. Methods Appl. Sci., 37 (2014), pp. 1392–1404.

[102] J. R. Silveira, A. G. Hughson, and B. Caughey, *Fractionation of prion protein aggregates by asymmetrical flow field-flow fractionation*, Methods Enzymol., 412 (2006), pp. 26–33.

[103] E. M. Sparrow, J. W. Ramsey, and R. G. Kemink, *Freezing controlled by natural convection*, ASME J. Heat Transfer, 101 (1979), pp. 578–584.

[104] H. Tang and Y. Fung, *Fluid movement in a channel with permeable walls covered by porous media - a model of lung alveolar sheet*, ASME J. Appl. Mech., 97 (1975), pp. 45–50.

[105] S. Tlupova and R. Cortez, *Boundary integral solutions of coupled Stokes and Darcy flows*, J. Comput. Phys., 228 (2009), pp. 158–179.

[106] J. M. Urquiza, D. N'Dri, A. Garon, and M. C. Delfour, *Coupling Stokes and Darcy equations*, Appl. Numer. Math., 58 (2008), pp. 525–538.

[107] D. Vassilev, C. Wang, and I. Yotov, *Domain decomposition for coupled Stokes and Darcy flows*, Comput. Methods Appl. Mech. Engrg., 268 (2014), pp. 264–283.

[108] R. Viskanta, *Mathematical modelling of transport processes during solidification of binary systems*, JSME Int. J. Ser. II, 33 (1990), pp. 409–423.

[109] V. R. Voller, *An overview of the modelling of heat and fluid flow in solidification systems*, in Modeling of Casting, Welding, and Advanced Solidification Processes V, M. Rappaz, M. R. Ozgu, and K. W. Mehin, eds., The Metallurgical Society, Warrendale, PA, 1991, pp. 661–675.

[110] W. Wang and C. Xu, *Spectral methods based on new formulations for coupled Stokes and Darcy equations*, J. Comput. Phys., 257, part A (2014), pp. 126–142.

[111] Y. Wu and B. Bai, *Efficient simulation for low salinity waterflooding in porous and fractured reservoirs*, in Proceedings of the SPE Reservoir Simulation Symposium, The Woodlands, TX, Society of Petroleum Engineers, 2009, Document ID 118830-MS.

[112] Y. Wu, G. Qin, R. E. Ewing, Y. Efendiev, Z. Kang, and Y. Ren, *A multiple-continuum approach for modeling multiphase flow in naturally fractured vuggy petroleum reservoirs*, in Proceedings of the International Oil & Gas Conference and Exhibition in China, Beijing, Society of Petroleum Engineers, 2006, Document ID 104173-MS.

[113] T. Zhang and J. Yuan, *Two novel decoupling algorithms for the steady Stokes-Darcy model based on two-grid discretizations*, Discrete Contin. Dyn. Syst. Ser. B, 19 (2014), pp. 849–865.

[114] L. Zuo and Y. Hou, *A decoupling two-grid algorithm for the mixed Stokes-Darcy model with the Beavers-Joseph interface condition*, Numer. Methods Partial Differential Equations, 30 (2014), pp. 1066–1082.

[115] L. Zuo and Y. Hou, *A two-grid decoupling method for the mixed Stokes-Darcy model*, J. Comput. Appl. Math, 275 (2015), pp. 139–147.